INORGANIC CHEMISTRY FRONTIERS

CCS 中国化学会 CHINESE CHEMICAL SOCIETY

ROYAL SOCIETY OF CHEMISTRY

Photofunctional transition metal complexes as cellular probes, bioimaging reagents and phototherapeutics

Journal:	*Inorganic Chemistry Frontiers*
Manuscript ID	QI-REV-07-2021-000931
Article Type:	Review Article
Date Submitted by the Author:	26-Jul-2021
Complete List of Authors:	Lo, Kenneth; City University of Hong Kong, Chemistry Xu, Guang-Xi; City University of Hong Kong, Department of Chemistry Mak, Eunice Chiu-Lam; City University of Hong Kong, Department of Chemistry

INORGANIC CHEMISTRY
FRONTIERS

CCS 中国化学会 CHINESE CHEMICAL SOCIETY

ROYAL SOCIETY OF CHEMISTRY

Inorganic Chemistry Frontiers publishes significant research at the interfaces between inorganic chemistry and related disciplines. Papers published in the journal should represent a significant development in the particular field judged according to originality, quality of scientific content and contribution to existing knowledge. Structural reports merely dealing with synthesis and characterization will not be considered.

Only work within the **top 20%** of the filed in terms of quality and interest should be recommended for publication.

Journal home page: http://rsc.li/frontiers-inorganic

*2019 Journal Citation Reports ®, (Clarivate Analytics, June 2020)

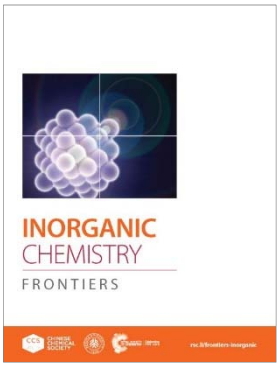

Impact Factor*
5.958

Reviews — Referee Guidelines

Review articles in *Inorganic Chemistry Frontiers* should

- provide a **critical** and **in-depth** discussion of a particularly relevant or interesting topic in inorganic chemistry
- aim to provide the reader with an **authoritative**, **balanced** and **up-to-date** overview, and not a comprehensive list of all possible references
- aim to identify areas in the field where **further developments** are needed

When assessing this manuscript please take the following into account:

- *Inorganic Chemistry Frontiers* Review-type articles undergo a **rigorous and full peer review** procedure, in the same way as regular research papers
- A Review Article is normally within **20** journal pages, together with supporting figures and tables. In all cases considerable flexibility on the length can be offered if justified.

Please provide your report rapidly and within **14 days**, or inform the Editor immediately if you cannot do so. We welcome suggestions of alternative referees. It is the expectation that **only work with two strong endorsements will be accepted** for publication.

Thank you very much for your assistance in evaluating this manuscript.

Inorganic Chemistry Frontiers
InorgChemFrontiersED@rsc.org

香港城市大學
City University of Hong Kong
專業 創新 胸懷全球
Professional·Creative
For The World

26 July 2021

Dr Zoey Yu
Deputy Editor
Inorganic Chemistry Frontiers

Dear Dr Yu,

Submission of manuscript

Thank you for your invitation of 22 June 2020. I apologize for my late submission. I am writing to submit a manuscript entitled “Photofunctional transition metal complexes as cellular probes, bioimaging reagents and phototherapeutics” to be considered for publication as a critical review in *Inorganic Chemistry Frontiers*.

In this critical review article, we have summarised the recent development of transition metal complexes (TMCs) in four selected major applications. First, we have discussed the applications of TMCs as intracellular sensors for biomolecules. Also, we have covered their potential as bioimaging reagents for intracellular microenvironment monitoring and specific organelle staining. Additionally, we have collected studies of the recent applications of TMCs as photosensitisers for photodynamic therapy and photoactivated chemotherapy. Finally, future development of TMCs for new diagnostic and therapeutic applications is also discussed. We believe that the review article will provide an in-depth and concise reference of the development of TMCs for specialists and newcomers to the fields alike. We are confident that it will be appealing to the wide and diverse readership of *Inorganic Chemistry Frontiers*.

The manuscript is not under consideration for publication and has not been published elsewhere in any medium including electronic journals and computer databases of a public nature.

Thank you for your attention.

Yours sincerely,

Kenneth Lo

--
Professor Kenneth Kam-Wing Lo
Department of Chemistry
City University of Hong Kong
Tat Chee Avenue
Hong Kong
P. R. China

Tel: (852) 3442 7231
Fax: (852) 3442 0522
E-mail: bhkenlo@cityu.edu.hk

Justifications for publication in *Inorganic Chemistry Frontiers*

In this critical review article, we have summarised the recent development of transition metal complexes (TMCs) in four selected major applications. First, we have discussed the applications of TMCs as intracellular sensors for biomolecules. Also, we have covered their potential as bioimaging reagents for intracellular microenvironment monitoring and specific organelle staining. Additionally, we have collected studies of the recent applications of TMCs as photosensitisers for photodynamic therapy and photoactivated chemotherapy. Finally, future development of TMCs for new diagnostic and therapeutic applications is also discussed. To ensure the timeliness of this review article, all the examples described were taken from the literature published in the last five years. We have focussed on the structural designs, photophysical and photochemical behaviour, cellular uptake properties, bioimaging applications, and photocytotoxic activity of a range of photofunctional TMCs. We believe that the review article will provide an in-depth and concise reference of the development of TMCs for specialists and newcomers to the fields alike. We are confident that it will be appealing to the wide and diverse readership of *Inorganic Chemistry Frontiers*.

Photofunctional transition metal complexes as cellular probes, bioimaging reagents and phototherapeutics

Guang-Xi Xu,[a] Eunice Chiu-Lam Mak[a] and Kenneth Kam-Wing Lo*[a, b, c]

[a]*Department of Chemistry, City University of Hong Kong, Tat Chee Avenue, Hong Kong, P. R. China. E-mail: bhkenlo@cityu.edu.hk*

[b]*State Key Laboratory of Terahertz and Millimetre Waves, City University of Hong Kong, Tat Chee Avenue, Hong Kong, P. R. China*

[c]*Centre of Functional Photonics, City University of Hong Kong, Tat Chee Avenue, Hong Kong, P. R. China*

Abstract

By virtue of their rich photophysical and photochemical properties, transition metal complexes (TMCs) have been extensively studied in multidisciplinary research. In this review, recent studies on TMCs for biological applications are described with a focus on the behaviour of TMCs as specific intracellular sensors and organelle-targeting imaging reagents. Some prominent examples of TMCs as photosensitisers for *in vitro* and *in vivo* phototherapies, such as photodynamic therapy and photoactivated chemotherapy, are highlighted. Also, future development of TMCs for new diagnostic and therapeutic applications is discussed.

1. Introduction

Transition metal complexes (TMCs) with d^6, d^8 and d^{10} electronic configurations have been widely used in catalysis, organic light-emitting diodes (OLEDs) and biological diagnosis because of their unique stereochemical, redox and electronic features.[1,2] In particular, the design of TMCs as imaging reagents in the visualisation of biological species and as therapeutic photosensitisers for photodynamic therapy (PDT) and photoactivated chemotherapy (PACT) has received considerable attention recently.[3-5]

During the past decade, optical imaging, as a non-invasive and low-cost technology, has emerged as an alternative modality for bioimaging.[6] Compared to traditional small molecule-based bioimaging probes, potential alternatives are TMCs since they display intriguing photophysical and photochemical features and are readily tunable based on the coordination of their ligands. Notably, the long luminescence lifetimes of TMCs eliminate the effects of light scattering and background autofluorescence (< 10 ns) in complex intracellular environments.[7,8] TMCs also

exhibit enhanced photostability and resistance to photobleaching even after long-term exposure to intense photoirradiation conditions.[9-10] The large Stokes shifts of TMCs can minimise self-quenching that is commonly found in organic dyes.[11]. Additionally, the photophysical properties of TMCs show environment-sensitive changes that are highly responsive in intracellular settings, such as pH,[13,14] hypoxia,[15,16] temperature,[17] polarity[18] and viscosity.[19,20] These remarkable properties render TMCs suitable reagents for intracellular bioimaging and biosensing.

TMCs offer advantageous characteristics as therapeutic reagents in medicinal chemistry. The coordination number of transition metal ions (usually 4, 5 and 6) enhances the structural diversity of the compounds, making them attractive "all-in-one" therapeutics.[21,22] The lipophilicity, electronic and steric properties of the complexes can be finely tuned by modifying the ancillary ligands, allowing the metal complexes with controllable cellular uptake efficiency, intracellular localisation, (photo)cytotoxicity, reactivity and selectivity towards specific tumours or tissues.[23,24] The diversity of excited states of TMCs make them ideal light-mediated photosensitisers for PDT or PACT with high spatial-temporal controllability.[25]

The applications of TMCs have been systematically described in some interesting reviews, with a specific focus on bioimaging, PDT, theranostics, etc.[26-28] In this review, we aim to summarise the development of TMCs in the last five years in the four most important applications. First, we discuss their applications as intracellular sensors for biomolecules. Next, we cover their bioimaging potential for intracellular microenvironment monitoring and specific organelle staining. Following, we collect some of their recent applications as PDT agents. Finally, the development of photosensitive metal complexes for PACT applications is discussed with a focus

on the different reaction mechanisms, such as photoreduction, ligand photocleavage, photosubstitution and photorelease of nitric oxide (NO) and carbon monoxide (CO).

2. Sensing of intracellular biomolecules

The design of cellular probes for detection and quantification of intracellular biomolecules with high sensitivity and selectivity is of utmost importance for regulating cellular functions and understanding the biological roles of biomolecules. In the presence of a distinct species, the probe reacts or binds with the species giving rise to specific photophysical changes, such as emission intensity and lifetime, which can be easily monitored by laser-scanning confocal microscopy (LSCM) and time-resolved phosphorescence lifetime imaging microscopy (PLIM).[29]

Biothiols, including cysteine (Cys), homocysteine (Hcy), glutathione (GSH) and hydrogen sulfide (H_2S), play a critical role in biological systems. These sulfur-containing compounds are important for maintaining intracellular redox activities via the equilibria between reduced free thiol and oxidised disulfide forms.[30] Abnormal levels of biothiols are associated with many diseases, including cardiovascular and neurodegenerative diseases and cancer. Cys is a thiol-containing amino acid residue that plays functional roles in protein synthesis, redox balance and metal trafficking.[31] The deficiency of Cys is related to diseases such as skin lesions, liver damage and edema.[31] Hcy is a homologue of Cys, and a high level of Hcy is relevant to cardiovascular and Alzheimer's diseases.[32] GSH is the most abundant Cys-containing biothiol in cells (*ca.* 2 – 10 mM) and serves as an endogenous antioxidant that protects cells against oxidative stress.[33] Abnormal levels of GSH are implicated in diseases such as liver damage, psoriasis and cancer.[34] H_2S, the simplest biothiol, is a gaseous species produced endogenously through both enzymatic and non-enzymatic processes. Although its essential role as a neurotransmitter has been known, anomalous levels of H_2S may contribute to neurodegenerative disorders such as Parkinson's and Alzheimer's diseases.[35] Lo and co-workers have reported cyclometallated iridium(III) complexes (**1** and **2**), and

a bimetallic iridium(III)-rhenium(I) complex (**3**) containing disulfide linkers, that serve as biological sensors for Cys, GSH and H_2S.[36] In particular, upon incubation with GSH at increasing concentrations, complex **3** exhibits obvious emission enhancement at 517 nm and reduction at 655 nm, with good linearity in the emission intensity ratio ($I_{517\ nm}/I_{655\ nm}$). The spectral response is ascribed to disulfide bond cleavage by GSH and subsequent inhibition of fluorescence resonance energy transfer (FRET) from the rhenium(I) to the iridium(III) moiety.

Apart from total biothiols detection, discrimination of biothiols is of great significance for correlating each of the biothiols with a particular subset of disease states. Zhang and co-workers have designed a phosphorogenic ruthenium(II) complex (**4**) for simultaneous total biothiol detection and biothiol discrimination.[37] The complex displays very weak emission intensity due to the incorporation of an electron withdrawing 7-nitro-1,2,3-benzoxadiazole (NBD) moiety that serves as a quencher by photoinduced electron transfer (PET). The conjugation of NBD to the complex through a responsive ether bond allows nucleophilic substitution by biothiols to liberate long-lived red-emitting ruthenium-OH, short-lived green-emitting NBD-NR for Cys/Hcy and non-emissive NBD-SR for GSH. The remarkable difference in luminescence colour response enables differentiation between GSH and Cys/Hcy by steady-state luminescence analysis (Fig. 1). The long lifetime of ruthenium-OH allows total biothiols detection by time-gated luminescence analysis that bypasses autofluorescence and NBD-NR fluorescence. Importantly, the high sensitivity and selectivity and good biocompatibility of complex **4** facilitate similar photophysical responses *in vitro* and *in vivo*. The development of phosphorogenic probes responsive to both total and individual biothiols can be utilised for future diagnosis and discrimination of diseases related to biothiols.

Formaldehyde is an important reactive carbonyl species that can be produced by metabolic processes in living cells and has implication for various diseases including cancers, diabetes and heart, liver and neurodegenerative disorders.[38] Elevated levels of endogenous formaldehyde in cancer cells have been shown to be a possible indicator of tissue cancerisation and tumour progression. The generation of endogenous formaldehyde is associated with lysosomes (pH 4.5 – 5.5) that play a significant role in metabolism.[39] The design of responsive probes that detect lysosomal formaldehyde would contribute to cancer diagnosis and treatment monitoring. To illustrate this, a ruthenium(II) complex bearing a 2,4-dinitrobenzene (DNB) unit (**5**) has been developed by Yuan and co-workers as a phosphorogenic probe for the detection and quantification of lysosomal formaldehyde.[40] The weak luminescence of the complex is attributed to PET quenching by the electron-withdrawing DNB unit. Upon reaction of the complex with formaldehyde in an acidic microenvironment, the DNB moiety is cleaved off, which is accompanied by enhanced emission intensity. Good linearity is observed between the luminescence intensity at 644 nm and the concentration of formaldehyde (0 to 650 μM). Steady-state and time-gated luminescence analyses of human sera and *ex vivo* mouse organs reveal the capability of complex **5** as a probe for the quantification of formaldehyde. Notably, this complex enables both *in vitro* and *in vivo* detection of formaldehyde, as performed by luminescence imaging of lysosomal formaldehyde of HeLa cells and monitoring of formaldehyde scavenging by $NaHSO_3$ in tumour-bearing mice.

Peroxynitrite ($ONOO^-$) is a short-lived reactive oxygen and nitrogen species (RONS) produced from the diffusion-controlled reaction of NO with superoxide anion radical ($O_2^{\bullet-}$). Excessive generation of $ONOO^-$ can contribute to various pathologies including cardiovascular and

neurodegenerative disorders and cancer.[41] Zhao and co-workers have reported the design of a near-infrared (NIR) phosphorescent polymeric probe (**6**) for the detection of $ONOO^-$ in intracellular microenvironment.[42] Upon addition of $ONOO^-$, the *N*-(4-hydroxylphenyl)rhodol-appended $ONOO^-$-sensitive iridium(III) complex undergoes *N*-dearylation reaction which releases the *N*-phenyl moiety, yielding a highly emissive complex. Photophysical studies reveal a gradual increase in the intensity of emission band at 680 nm and negligible change at 600 nm with the increase in $ONOO^-$ concentration, giving rise to significant enhancement in the emission intensity ratio ($I_{680\ nm}/I_{600\ nm}$) and extended lifetimes of the complex. The probe has also been employed to detect $ONOO^-$ levels in live RAW 264.7 cells and inflamed mice by ratiometric and time-resolved photoluminescence imaging with a high signal-to-noise ratio. In particular, the probe has illustrated the elevated intracellular generation of $ONOO^-$ in drug-induced liver injury, which may provide a possible explanation to the mechanism of drug-induced hepatoxicity.

Hypochlorous acid (HClO)/hypochlorite (ClO^-) is a reactive oxygen species (ROS) that is generated via oxidation of chloride by hydrogen peroxide under the catalysis of heme enzyme myeloperoxidase (MPO) in biological systems. At normal concentrations, ClO^- kills a range of pathogens and is vital for the regulation of the immune defense system. However, higher levels of ClO^- are known to be involved in atherosclerosis, cancers and cardiovascular and neurodegenerative diseases.[43] To detect ClO^- in live cells, Lv and co-workers have designed a two-photon NIR iridium(III) complex appended with a diaminomaleonitrile moiety (**7**), which serves as a phosphorogenic probe for multi-signal detection and multimodal imaging of ClO^-.[44] The complex exhibits weak emission due to non-radiative decay associated with the C=N bond in the excited state and the presence of an electron-withdrawing diaminomaleonitrile. Upon reaction with

ClO^-, the C=N bond is oxidised to carboxylate, resulting in significant emission enhancement and lifetime extension. A linear correlation between the lifetime of complex **7** and the concentration of ClO^- allows the quantification of ClO^-. The probe is applicable for two-photon imaging, with maximum two-photon absorption (TPA) cross-section of 97 GM at 800 nm in the presence of ClO^-. Importantly, complex **7** allows the visualisation of ClO^- in living cells, tissues and inflammatory mouse models, demonstrating its potential as a ClO^- probe in living systems.

Caspase-3 is a fundamental enzyme that is required for normal brain development and plays a crucial role in apoptosis-induced cell death.[45] Over-activation of caspase-3 can cause neurodegenerative diseases such as Alzheimer's disease.[46] Recently, Huang and co-workers have designed a phosphorescent iridium(III) complex appended with dibenzocyclooctyne (DBCO) (**8**) to detect the catalytic activity of caspase-3 in aqueous solutions and cisplatin-stimulated apoptotic cells through the bioorthogonal "labelling after recognition" strategy.[47] A tetrapeptide motif Asp-Glu-Val-Asp (DEVD) modified with azide and norbornylene chemical reporters at the amino and carboxyl termini respectively is chosen as the caspase-3-cleavable substrate. Upon bis-labelling of the peptide motif via strain-promoted alkyne-azide cycloaddition between DBCO and azide and inverse electron-demand Diels-Alder reaction between rhodamine-modified tetrazine and norbornylene, intramolecular FRET occurs from complex **8** to the rhodamine moiety, leading to quenched emission lifetime of the complex. The emission lifetime of the complex is substantially elongated upon peptide cleavage by caspase-3, which can be employed as an indicator for monitoring catalytic activity of caspase-3 via PLIM (Fig. 2). This approach offers lifetime responses with higher sensitivity and efficiency, due to reduced steric hindrance and non-specific interactions that have typically been observed in "labelling before recognition" sensing method.

3. Monitoring of cellular microenvironment

The dynamic nature of the cellular microenvironment is governed by physical factors such as oxygen level, pH, viscosity and temperature. Abnormalities of these factors may disrupt cellular functions and result in a diverse range of diseases. Therefore, it is important to study these factors to understand their impact on cellular processes including molecule trafficking and signalling.

Molecular oxygen is an essential molecule for cellular respiration and sustaining life. Insufficient and excessive oxygen supply, referred to as hypoxia and hyperoxia respectively, are indicators of pathological conditions. Hypoxia is a general feature of many diseases such as pulmonary disease and cancer,[48] whereas hyperoxia may lead to excess generation of RONS that cause irreversible oxidative damage to cells and tissues.[49] Iridium(III) complexes with or without aminomethyl groups on their cyclometallating ligands (**9**) have been studied by Huang and co-workers.[50] In particular, complex **9f** containing piperidinomethyl substituted cyclometallating ligands is capable of differentiating among hypoxic, normoxic and hyperoxic conditions in live cells and *in vivo*. The complex exhibits dual phosphorescence with comparable intensities in aqueous buffer under ambient conditions. This is attributed to the incorporation of non-conjugated amino groups in the cyclometallating ligands that gives rise to additional electronic transitions from the lone pairs to the π*(N^N) orbitals, resulting in a new ^{3}NLCT excited state ($n \rightarrow \pi^*$) that inhibits internal conversion between the ^{3}IL and ^{3}CT states. A ratiometric spectral response is observed upon changing the oxygen content, affording distinguishable green, orange and red emission in aqueous solution under an atmosphere of nitrogen, air and oxygen, respectively. Remarkably, the complex allows real-time intracellular oxygen sensing in HepG2, HeLa and 3T3 cells with sensitive spectral

response towards both hypoxia and hyperoxia environments, and has been further applied to oxygen sensing in living mice.

Intracellular viscosity is a critical environmental factor to regulate diffusion-mediated cellular processes including metabolism, signalling pathways, transport and interactions between biomacromolecules in cellular membrane. Abnormal changes in intracellular viscosity are related to various diseases such as atherosclerosis, diabetes and neurodegenerative disorders.[51] Viscosity in the mitochondrial matrix plays a crucial role in network organisation, metabolite diffusion and metabolism. Iridium(III) complexes containing rotatable groups (**10**) have been developed by Mao and co-workers as mitochondria-targeting viscosity probes.[52] Among them, complex **10f** displays viscosity-dependent phosphorescence intensities and lifetimes, which are mainly the result of rotatable aromatic rings on the diphosphine ligand and rotatable aldehyde groups on the cyclometallating ligands. A linear relationship is obtained between the lifetime of the complex and solvent viscosity parameters. Under restricted microenvironments, molecular rotations become restricted and the emission lifetime is enhanced. Additionally, the complex can detect and quantify dynamic changes in mitochondrial viscosity selectively in real-time by two-photon PLIM (Fig. 3), with a maximum TPA cross-section of 444 GM at 750 nm. A time-dependent increase in the average emission lifetime is observed in complex **10f**-treated A549 cells as viscosity increases from about 35 to 100 cP. Similar lifetime response to viscosity changes has also been recorded for zebrafish imaging.

4. Staining of subcellular organelles

A eukaryotic cell is composed of cytoplasm containing different organelles, such as mitochondria, lysosomes, nucleus, endoplasmic reticulum (ER) and Golgi apparatus, enclosed within the plasma

membrane. These subcellular organelles are all of great significance in maintaining cellular functions and can be visualised selectively through staining with fluorescent organic dyes and luminescent lanthanide complexes. In recent years, there has been rising interest in the development of transition metal complexes as novel bioimaging reagents.

The plasma membrane consists of a phospholipid bilayer embedded with proteins that function as channels and transporters of ions and small molecules across the membrane. It serves as a barrier between the extracellular and intracellular environments and protects subcellular organelles within the cytoplasm.[53] Phosphorescent iridium(III) complexes bearing two lipophilic alkyl chains of different lengths (**11**) that stain the plasma membrane to different extents have been reported by Huang and co-workers.[54] The complexes are partially retained in the cell membrane during their cellular uptake in HeLa cells, owing to lipophilic interactions with the phospholipid bilayer that reduce internalisation of the complexes into the cells, and a higher extent of membrane staining is observed for complexes with longer carbon chains. Complex **11c** has been further utilised for sensing and distinguishing between endogenous and exogenous analytes due to its comparable distribution in the cell membrane and cytoplasm. Similarly, a ruthenium(II) complex appended with two lipophilic alkyl chains that have specific binding affinity to the cell membrane (**12**) has been reported by Zhao and co-workers.[55] Co-staining experiments with membrane-staining dye, DiO, reveal plasma membrane staining in HeLa cells. Interestingly, the complex displays good membrane-staining ability in cancer cells but weak luminescence and negligible membrane staining in normal cells, as demonstrated in A549 cancer cells, and HSF and 3T3 normal cells, respectively. This may be explained by the presence of anionic lipids and molecules that interact with the cationic complex in cancer cell membranes.

Mitochondria play a vital role in cellular stress responses including autophagy and apoptosis. Dysfunction of mitochondria may cause diverse diseases such as neurodegenerative and metabolic disorders and cancer.[56] Lo and co-workers have designed environment-sensitive luminescent iridium(III) complexes containing a sydnone moiety (**13**) as mitochondrial targeting probes via boorthogonal reaction.[57] Reaction of the sydnone complexes with (1*R*,8*S*,9*s*)-bicyclo[6.1.0]non-4-yn-9-ylmethanol (BCN-OH) leads to enhanced emission intensity, because of the formation of less polar pyrazole derivative after the specific bioorthogonal reaction between the sydnone moiety and BCN unit. Importantly, upon incubation of the complexes with a BCN-BSA conjugate, the complexes exhibit pronounced emission enhancement (I/I_o = up to 24.9) and extended lifetime compared to that of BCN-OH unit, due to the rigid and hydrophobic environment offered by BSA protein. Intracellular distribution studies show that the HeLa cells treated with BCN-modified ceramide (Fig. 4a) and complex **13b** display enhanced emission intensity at the mitochondria (Fig. 4b and c), due to the high lipophilic and cationic character of the luminescent adduct. Keyes and co-workers have reported a ruthenium(II) light-switching complex appended with a mitochondrial penetrating peptide (**14**) that displays specific targeting capability of mitochondrial nucleoids.[58] The dppz ligand acts as a molecular light switch upon intercalation with mitochondrial DNA. LSCM images reveal rapid cellular uptake of complex **14** and display punctate staining in the mitochondria, with good co-localisation with MitoTracker Deep Red. Additionally, binding to mitochondrial DNA by complex **14** has been further validated with resonance Raman and luminescence lifetime imaging.

Lysosomes are membrane-bound organelles that contain multiple acid hydrolases. These enzymes decompose extracellular and intracellular materials that have been internalised by endocytosis and sequestered by autophagy respectively.[59] Lysosomes are also involved in various cellular processes including cell signalling, metabolism and apoptosis. Lysosomal dysfunction may contribute to lysosomal storage, neurodegenerative and metabolic diseases and cancer.[60] Lo and co-workers have reported three phosphorogenic rhenium(I) complexes (**15**) carrying a sydnone moiety for bioorthogonal labelling of lysosomes.[61] Due to the quenching potential of the sydnone unit, the complexes exhibit weak emission intensity, but significant emission enhancement upon treatment with strained alkynes such as BCN derivatives. The bioorthogonal ligation of complex **15a** with a BCN-modified morpholine (BCN-morph) has been visualised in HeLa cells. Co-localisation studies show strong lysosomal labelling, demonstrating the immense potential for development of diverse phosphorogenic bioorthogonal probes for labelling of subcellular organelles. In another study, Zhang and co-workers have designed an iridium(III) complex (**16**) that enables long-term lysosome tracking via pH-responsive self-assembly-induced emission in aqueous solutions at low concentrations.[62] The emission is ascribed to π-π stacking oriented self-assembly through conjugation of two aromatic peptide-based functionalities (naphthalene-Phe-Phe-Lys (NapFFK)). Endocytic uptake is enhanced by capping the C-terminal of each NapFFK with taurine, an aminosulfonic acid, to attain a non-hydrolyzable probe. Through endocytic trafficking, the acidic microenvironment (pH 4.5 – 5.5) in lysosomes stimulates irreversible self-assembly of the complex from nanoparticles into sturdily packed networks by π-π interactions. Upon treatment of HeLa cells at passage 0 with the complex at low concentration and subsequent excitement at 488 nm, fluorescent images reveal continuous emission for over 15 generations (Fig. 5a and b). At passage 14, the lysosome labelling rate is still maintained with only a mild decline

in emission intensity, as shown in Fig. 5c, indicating its outstanding performance for long-term lysosome tracking with high photostability and biostability.

In eukaryotic cells, the nucleus is separated from the cytoplasmic compartment by the nuclear envelope, which is a double membrane permeated with nuclear pore complexes that enable exchange of macromolecules, such as histones, transcription factors and RNAs, between the nucleus and cytoplasm. It contains most of the genetic material, DNA, and plays a major role in the control of cellular activities by regulating gene expression and mediating DNA replication during the cell cycle. Dysfunction in the nucleus causes serious damage to cellular functions and even cell death.[63] Recently, three phosphorescent iridium(III) complexes (**17**) have been designed by Pope and co-workers to investigate the cellular translocalisation characteristics of a c-Myc signal peptide in cells.[64] Complex **17c** containing a c-Myc signal peptide is essentially non-cytotoxic, compared to its non-peptide analogue (**17b**) which induces mitochondrial dysfunction at low concentrations. Cell imaging studies illustrate the increased nuclear staining upon increasing concentrations of complex **17c** in human fibroblast cells as confirmed by good co-localisation with Hoechst 33342. The nuclear localisation of complex **17c** is mainly attributed to the incorporation of the nuclear localisation (NLS) peptide sequence (PAAKRVKLD). Salvati and co-workers have reported a phosphorescent ruthenium(II) tris-phenanthroline complex conjugated to a linear polycationic polyamidoamine (PAA) (**18**) that shows light-triggered trafficking to the cell nucleus.[65] Upon treatment with complex **18** at low concentrations with continuous illumination, HeLa cells show a gradual increase of nuclear emission signal over time, compared to the non-illuminated cells. The light-triggered nuclear translocation is due to singlet oxygen ($^1O_2$) generation by the complex which causes nuclear membrane damage. Two nucleus-targeted

dinuclear ruthenium(II)-rhenium(I) dppz complexes linked by different linkers (**19**) have been investigated by Thomas and co-workers.[66] Complex **19a** displays strong luminescence signal from nucleus at all concentrations, while complex **19b** containing an *N*,*N*'-bis(4-pyridylmethyl)-1,6-hexanediamine tether ligand shows concentration-dependent intracellular localisation in A2780 cells. At concentrations lower than the IC_{50} value (11 μM), punctuate staining is observed throughout the cytosol with preferential accumulation in lysosomes and mitochondria, but at higher concentrations, evident nuclear staining results. The localisation dynamics have been confirmed by stimulated emission depletion microscopy.

5. Photodynamic therapy

PDT as a photoactivatable and non-invasive strategy has emerged as a promising therapeutic modality for diseases and cancer treatment. In general, PDT uses a combination of photosensitisers and light to convert the non-toxic molecular oxygen to cytotoxic ROS and induce severe oxidative damage to intracellular biomolecules, leading to apoptosis- or necrosis-mediated cancer cell death.[67] Many photosensitisers, such as porphyrins, chlorins, phthalocyanines and their structural derivatives, have been developed. These compounds have drawbacks such as photosensitivity for patients and the need for high dosages.[68] Regarding the long-lived triplet excited state, efficient $^1O_2$ generation behaviour, good photostability and controllable cytotoxicity, recently, phosphorescent TMCs, such as rhenium(I), ruthenium(II) and iridium(III) polypyridine complexes, have been explored as potential photosensitisers for PDT.[69,70] Notably, a ruthenium(II) polypyridine complex, TLD1433, designed by McFarland and co-workers is under phase II human clinical trials.

5.1 Type I-based photodynamic therapy

Hypoxia is a common native tumour microenvironment (TME) because of the limited oxygen diffusion, rapid cell proliferation and unstable blood supply in tumours microvascular networks,[71,72] which seriously affects the efficiency of oxygen-dependent therapeutics. Oxygen-independent type I-based PDT is a promising strategy to overcome hypoxia limitation. In general, proton or electron transfer occur between the photosensitisers and intracellular biomolecules upon photoirradiation, leading to the generation of cytotoxic ROS, such as $O_2^{\bullet-}$, hydroxyl radical (•OH) and hydroperoxyl radicals ($\bullet HO_2$). Two luminescent cationic iridium(III) complexes with different N^N ligands (**20**) have been reported by Elias and co-workers for PDT under hypoxic conditions.[73] Due to the positive charge, the complexes are rapidly uptaken by the cells and exhibit mitochondrial accumulation behaviour. Incubation of the complexes with different cancer cell lines under both hypoxic and normoxic conditions shows relatively low cytotoxicity but higher photo-induced cytotoxicity upon photoirradiation. Notably, complex **20b** exhibits a higher hypoxia/normoxic IC_{50} ratio and lower $^1O_2$ generation efficiency than complex **20a**. Additionally, complex **20b** displays potent photo-induced destruction of the hypoxic spheroids, demonstrating promising anticancer activity of complex **20b** through type I process under low oxygen conditions.

Ruiz and co-workers have reported ruthenium(II) heteroleptic complexes (**21**) as novel photosensitisers for type I-based PDT through the generation of multiple cytotoxic radicals under hypoxic environments.[74] Upon photoirradiation under normoxic conditions, all the complexes display moderate photocytotoxicity towards HeLa cells with poor PI values (1.6 – 76.3 fold). However, when the intracellular oxygen level is lower than 2%, enhanced photo-induced cytotoxicity is observed for complexes **21b** and **21d**, with PI values up to 769 and 588 fold,

respectively. The potent anticancer efficiency is ascribed to the production of •OH and H_2O_2, resulting in the inhibition of protein translation and apoptosis-induced cancer cell death.

Luminescent ruthenium(II) complex containing a light-harvesting coumarin unit (**22a**) and its coumarin-free counterpart (**22b**) have been synthesised for PDT applications.[75] Compared to complex **22b**, complex **22a** displays a weaker emission intensity and a low $^1O_2$ quantum yield, but a high photocytotoxic response under low oxygen conditions upon photoirradiation and induces substantial cancer cell death via mitochondrial damage. Additionally, this photocytotoxic effect is prominent in hypoxic 3D multicellular spheroids. Density functional theory (DFT) calculation studies indicate that the effective type I-PDT efficiency of complex **22a** is attributable to the combination of metal complex and coumarin moiety, facilitating the direct electron transfer from the complex to the surrounding substrate to generate cytotoxic ROS.

5.2 Type II-based photodynamic therapy

Type II-based PDT is regarded as the primary photosensitisation mechanism in PDT. In contrast to type I-based PDT, the photoreaction procedure for type II-based PDT involves the energy transfer from photosensitisers at the first triplet excited state (T_1) to surrounding triplet molecular oxygen ($^3O_2$) to generate excessive levels of cytotoxic $^1O_2$, which ultimately leads to the death of cancer cells and inhibition of tumour growth.[76]

The structural configuration, lipophilicity, photophysical properties and intracellular localisation of transition metal complexes greatly affect their PDT efficiency.[70,77,78] Lo and co-workers reported phosphorogenic nitrone-appended iridium(III) complexes (**23**) with controllable emission enhancement and $^1O_2$ generation efficiency through a bioorthogonal approach.[79] These complexes

display weak emission and $^1O_2$ generation quantum yields due to the efficient quenching effect from the C=N photoisomerisation from the nitrone unit. After incubation with BCN derivatives, the complexes exhibit substantially enhanced emission intensity (up to 327.1 fold) with higher $^1O_2$ quantum yields as a result of the strain-promoted alkyne-nitrone cycloaddition reaction between nitrone and BCN derivatives to form non-quenching isoxazoline derivatives. The addition of complexes **23** to SNAP-tag expressing Chinese hamster ovary (CHO)-K1 cells that have been pretreated with benzylguanine-modified BCN (BG-BCN) leads to potent photocytotoxicity with a pronounced increase in photocytotoxicity index (PI) to 9.0 – 115.9 relative to that of the non-BCN-BG pretreated groups. These promising results demonstrate that the combination of bioorthogonal reaction and protein tag technology has great potential as PDT-based theranostic agents.

To investigate the effects of ligand coordination of TMCs on phototherapeutic efficiency, Sun and co-workers have designed iridium(III) bis(terpyridine) complexes with different substitutions at the 4-position of tpy (**24**).[80] Complexes **24b** – **f** conjugated with different electron-donating substituents display broad absorption profiles from visible to NIR regions. Notably, complex **24d** containing a pyrenyl substituent shows a long transient absorption lifetime (5.8 μs) with a high $^1O_2$ quantum yield (Φ_Δ = 0.81) and lower cytotoxicity towards Human Melanoma (SK-MEL-28) cancer cells. Upon photoirradiation, complex **24d** displays pronounced photocytotoxicity against SK-MEL-28 cancer cells with an apparent therapeutic effect (PI > 1652). Complex **24d** inhibits the growth of solid tumours in xenograft tumour mice model after photoirradiation with no significant effect on body weight.

To improve the emission intensity and $^1O_2$ generation efficiency, an iridium(III) complex

conjugated with human serum albumin (HSA) has been synthesised by Sadler and co-workers using maleimide-modified iridium(III) complex (**25**) as the parent complex.[81] Facile bioconjugation of complex **25** leads to strong emission enhancement with a high emission quantum yield and extended emission lifetime compared to its HSA-free counterpart, which is attributed to the formation of hydrophobic local environments of the complexes after conjugation. Additionally, the HSA-modified complex exhibits a strong $^1O_2$ quantum yield. Cellular studies show that the conjugate is first localised in the cytoplasm, but increasing incubation time leads to nuclear localisation. Upon irradiation by visible light, the iridium(III)-albumin bioconjugate exhibits a strong PDT effect on different cancer cell lines and multicellular spheroids. In another study, luminescent iridium(III) complexes (**26** and **27**) modified with peptides have been synthesised and studied for their bioconjugation effects on PDT efficiency.[82] The complexes are tethered to a perfluorobiphenyl moiety, a molecule highly specific to the Cys of the π-clamp peptide (FCPF). The addition of the FCPF sequence to different organelle-targeting peptides would allow the conjugation of the complexes with relative ease. The resulting peptide conjugates exhibit different intracellular localisation behaviour based on the appended peptide sequence and a higher photocytotoxic effect than the peptide-free complexes.

5.3 NIR light-activatable photodynamic therapy

Most TMCs-based photosensitisers are excited by UV-visible light, the wavelength of which is shorter than the promising biological transparency window (600 – 900 nm), leading to limited tissue penetration and potential photo-induced damage to ambient tissues, thereby hindering their clinical translation. Hence, there is an urgent need for the design of metal complexes-based photosensitisers with strong red to NIR light absorption capability while maintaining their PDT

efficiency.

5.3.1 Two-photon excitation photodynamic therapy

Two-photon excitation (TPE) is a phenomenon in which the photosensitiser is simultaneously excited by two photons equal to the bandgap of the photosensitisers. TPE offers several advantages; for example, high spatial resolution, negligible physiological damage and increased tissue penetration depth.[78,83] These various features make TPE an attractive approach for anticancer PDT. Due to the efficient visible light absorption performance, good photostability and high two-photon absorption cross-section,[84] TMCs-based photosensitisers have been regarded as possible red to NIR light-activatable TPE PDT reagents.

A heterometallic ruthenium(II)-platinum(II) metallacycle (**28**) has been designed as a potential TPE photosensitiser.[85] The specific metallacycle structure confers complex **28** a red-shifted emission wavelength and high two-photon absorption cross-section of 1371 GM. The positive charge and enhanced lipophilicity allow complex **28** to exhibit dual localisation in nuclei and mitochondria of A549 cells. Treatment of complex **28**-loaded A549 cells with two-photon irradiation (λ_{ex} = 820 nm) induces remarkable cancer cell death attributable to the increased levels of intracellular $^1O_2$. Additionally, *in vivo* assays indicate that complex **28** can efficiently inhibit the growth of solid tumours with minimal side effects in A549 tumour-bearing nude mice.

The TPE efficiency of TMCs can be fine-tuned by expanding the conjugation of the coordination ligand or modifying it with specific functional groups. Recently, *trans*-stilbene, a well-known two-photon dye, has been adopted by Gasser and co-workers to be incorporated into ruthenium(II) polypyridine complexes (**29**) in order to extend the ligand conjugation.[86] Due to the strong two-

photon absorption property of the *trans*-stilbene unit,[87] the ruthenium(II) complexes show exceptionally high two-photon absorption cross-section (up to 6800 GM). Upon two-photon irradiation, complex **29g** displays obvious photo-induced cytotoxicity towards various monolayer cancer cells by oxidative damage of nuclei and mitochondria, giving rise to apoptosis-induced cancer cell death. Also, complex **29g** reveals substantial antitumour efficiency towards doxorubicin-resistant human colon cancer tumour after continuous irradiation.

Cyclometallated iridium(III) complexes have been conjugated to triphenylamine (**30**) and used as TPE photosensitisers for PDT through aggregation-induced emission (AIE) activation pathway.[88] Complexes **30a** – **c** display very weak emission intensities and low $^1O_2$ generation quantum yields in organic solvents. Upon changing to an aqueous medium, the iridium(III) complexes exhibit a dramatically enhanced emission intensity and $^1O_2$ generation efficiency due to the formation of highly emissive aggregates (Fig. 6a and b). The complexes show noticeable photocytotoxicity against HeLa cells than non-cancerous L02 cells with a PI value of 75. Notably, with respect to the limited tissue penetration of the one-photon excitation PDT strategy, the largest two-photon-absorption cross-section behaviour (Fig. 6c) affords complex **30a** enhanced phototherapeutic efficacy towards 3D multicellular tumour spheroids at low dosages upon two-photon irradiation.

5.3.2 Organic chromophore-metal conjugates for photodynamic therapy

The combination of TMCs with NIR light-harvesting organic chromophores, for example, porphyrin, cyanine and boron-dipyrromethene (BODIPY), is another straightforward approach to achieve NIR light-activatable PDT. The heavy atom effect from TMCs promotes intersystem crossing and prolongs the triplet state lifetime of the chromophore-metal conjugates, thereby

enhancing the PDT performance of the photosensitisers.

The exploration of cyanine and its derivatives as therapeutic and bioimaging reagents in biomedical field is well established owing to their strong NIR absorption, excellent biodegradability and biocompatibility properties.[89,90] Yang and co-workers have designed an iridium(III) complex (**31**) coordinated to a cyanine moiety to achieve intense NIR absorption.[91] The complexes self-assemble to yield nanoparticles with good photostability and water solubility while maintaining efficient $^1O_2$ generation capability (Fig. 7a).[92] Phototoxicity studies reveal obvious cell death of 4T1 cells, and concentration-dependent studies indicate a decrease in cell viability from 65.5 to 26.7%. The nanoparticles are readily uptaken by tumours through an enhanced permeability and retention effect, and are capable of tumour ablation compared to the control groups in the dark condition. Additionally, upon excitation by a pulsed laser, a strong photoacoustic signal is observed for the nanoparticles-treated cancer cells and shows a good linear relationship with the concentration of the nanoparticles, which affords the possibility for photoacoustic imaging. The nanoparticles serve as ideal theranostic agents for anticancer therapy (Fig. 7b).

Owing to the adjustable $^1O_2$ generation efficiency, diverse reactivity and strong visible-to-NIR absorption characteristics, BODIPY derivatives conjugated with TMCs have been investigated by some researchers.[92-94] Given the prominent $^1O_2$ quantum yield of $[Ru(bpy)_3]^{2+}$, recently, Chao and co-workers have designed an NIR-absorbing Ru-BODIPY conjugate (**32**) as a lysosome-specific photocytotoxic agent using $[Ru(bpy)_3]^{2+}$ as the parent complex.[95] Because of the direct π-conjugated coupling between the ruthenium(II) complex and distyryl-BODIPY moiety, complex

32b displays an apparent red-shift absorption (λ_{abs} = 652 nm) compared to that of the BODIPY-free counterpart (complex **32a**) and the free distyryl-BODIPY ligand. Cellular studies indicate that complex **32b** is preferentially accumulated in lysosomes and can induce apoptosis in various cancer cell lines after NIR light irradiation. Complex **32** exibits a high PI value of 3448 towards A375 cancer cells, due to the release of lysosomal proteases into the cytoplasm.

6. Photoactivated chemotherapy

Photoactivated chemotherapy (PACT) is an oxygen-independent phototherapy that is considered to be another promising light-mediated anticancer approach. The cytotoxicity of PACT agents can be finely modulated by releasing molecules of interest, for example, fluorescent probes, gasotransmitters and synthetic precursors. The release of these compounds is controllable, resulting in the conversion of prodrugs to biologically active species. An early TMCs-based photoactivatable chemotherapeutic agent $[Rh(bpy)_2Cl_2]Cl$ was reported in the 1990s,[96] followed by platinum-based photoactivatable metal complexes that have been developed for anticancer treatment.[97] The utilisation of rhenium(I), ruthenium(II), iridium(III) and platinum(IV) complexes for PACT has been well documented and comprehensively reviewed previously by Sadler,[98,99] Bonnet,[100,101] Turro[102], Ford[103,104] and co-workers. In general, TMC-based PACT agents can be divided into two groups based on their reaction mechanisms; photoreduction and photorelease.

6.1 Photoreduction

The relatively inert metal complexes, such as platinum(IV)[105,106] and cobalt(III),[107] can be permanently reduced through intracellular electron transfer upon light irradiation, because of their unique redox properties.[108] This results in the generation of highly reactive species with

controllable photocytotoxicity and enhanced therapeutic efficiency. For example, the light-mediated reduction of a *trans*-platinum(IV)-based complex (**33**) has been reported by Brabec and co-workers as a means to photoactivate the therapeutic prodrug for anticancer treatment.[109] Upon visible light excitation, the non-cytotoxic complex is reduced to a biologically active platinum(II) species with strong DNA binding ability, accompanied by the photogeneration of cytotoxic RONS. Additionally, the platinum(II) complex attacks intracellular proteins including the ROS-resistant enzyme thioredoxin reductase, leading to increased ROS damage and ER stress and thereby autophagy. The synergistic action of DNA damage and autophagy caused by the reactive platinum(II) complex induces enhanced immunogenic cell death.

6.2 Photorelease

Different from photoinduced metal reduction, light-mediated release of biologically active compounds is another innovative photoactivatable chemotherapeutic strategy.

6.2.1 Ligand photocleavage

Photoirradiation can induce the cleavage or rearrangement of chemical bonds. Thus, it is possible to temporarily inhibit the activity of metal complexes under physiological conditions by appending photocleavable protecting groups. Upon exposure to light irradiation, irreversible bond cleavage occurs, leading to deprotection of the metal complexes and restoration of their biological activities.

Poly(ethylene glycol) (PEG) chain modification can reduce the interaction of metal complexes with intracellular proteins, enzymes and DNA fragments, leading to a substantial decrease in cytotoxicity while retaining biological activities of the probes.[110] In the recent past, Lo and co-

workers have designed iridium(III) complexes (**34**) containing a nitrobenzyl-modified PEG pendant as mitochondrial targeting photoactivatable anticancer drugs for PACT (Fig. 8).[111] Owing to PEGylation, complex **34a** displays good biocompatibility (IC_{50} = 65.9 ± 5.7 μM) in the dark conditions compared with its PEG-free complex **34d** (IC_{50} = 0.4 ± 0.1 μM). Upon photoirradiation, the nitrobenzyl-modified protecting group on complex **34a** undergoes dissociation and releases the PEG tail, leading to noticeably enhanced cytotoxicity towards HeLa cells (IC_{50} = 1.4 μM). Notably, the PEGylated complex **34a** and PEG-free complex **34d** show negligible $^1O_2$ generation under irradiation conditions used in intracellular environments, illustrating that the enhanced cytotoxicity of the PEGylated complexes originates from an oxygen-independent ligand photocleavage pathway.

Hartman and co-workers designed a cyanine-appended platinum(II) complex (**35**) with high photo-induced cytotoxicity towards various cancer cells under the combined effect of PACT and PDT.[112] Conjugation with a cyanine moiety confers on the complex strong absorption and emission characteristics in the NIR region. After exposure to NIR light, the Pt–O bond dissociates producing bioactive platinum(II) species and cytotoxic $^1O_2$. Treatment of complex **35**-loaded cells with NIR light induces pronounced apoptosis-induced cell death compared to the cells incubated in dark conditions. LSCM studies demonstrate that light irradiation promotes migration of the complex from cytoplasmic organelles to nuclear DNA, indicating that the light-mediated cytotoxicity is presumed to be caused by the generated cytotoxic $^1O_2$ and the interaction between the bioactive platinum(II) species and DNA.

6.2.2 Photosubstitution

TMCs of the d-block elements with an accessible triplet metal-ligand charge transfer (^{3}MLCT) state show specific photo-substitution activity with intracellular environments. Upon photoactivation, the inactive metal complexes can create a ^{3}MLCT state, which subsequently interconverts to the low-lying dissociative d-d state, resulting in the substitution of the monodentate or bidentate ligands by solvent molecules.

Wu and co-workers reported a novel PEGylated ruthenium(II) complex $[Ru(Biq)_2(Hob)_2]PF_6$ (**36**) as a photosubstituted therapeutic agent.[113] In an aqueous solution, different hydrophobicity between the PEG chain and the ruthenium(II) complex allows the complex molecules to form nanoparticles with good biocompatibility and cellular uptake efficiency (Fig. 9a). The nanoparticles exhibit strong absorption profile in the red light region and upon subsequent exposure to red light irradiation, the nanoparticles release cytotoxic PEG-free complex $[Ru(Biq)_2(H_2O)_2](PF_6)_2$ and $^1O_2$. The release leads to pronounced anticancer performance in HeLa, HepG2 and PC3 cells (Fig. 9b – e). Phototherapy experiments with mice models demonstrate that the tumour size volume of mice treated with PEGylated nanoparticles decreases significantly with minimal pathological tissue damage after photoirradiation.

Three ruthenium(II)-based anticancer agents bearing a π-expansive bidentate ligand (**37**) that exhibit dual PACT and PDT behaviour have been proposed by Kodanko and co-workers.[114] Upon visible light irradiation, the pyridine ligand on the complexes is exchanged by solvent molecules, resulting in the release of ruthenium(II) complexes with strong DNA binding affinity. Notably, the long excited-state lifetimes (46 – 50 μs) give the complexes a good $^1O_2$ generation efficiency. Upon green-light excitation, the complexes show enhanced photoinduced cytotoxicity towards

prostate and breast cancer cells, triggering necrosis-mediated cell death, as evidenced by time-dependent photocytotoxicity studies.

Photoactivation of TMC-caged cytotoxic organic fragments displays potential anticancer effects. In this context, the cytotoxicity of a photolabile ruthenium(II)-caged rigidin analogue (**38**) has been systematically studied by Bonnet and co-workers using a photosensitive $[Ru(tpy)(bpy)](PF_6)_2$ as the parent complex.[115] Complex **38** exhibits lower cytotoxicity in the dark conditions, but upon irradiation with green light, the rigidin analogue is released and shows potent lung cancer cell proliferation reduction under both normoxic and hypoxic conditions through inhibition of tubulin polymerisation, which is comparable to that of free rigidin. Complex **38** efficiently inhibits the growth of tumours in nude mice xenograft models without causing adverse effects after PACT.

Abiraterone (ABI) is a well-known anticancer drug that can specifically bind to the CYP17A1 active site in specific cancer cell types to prevent androgen production. Recently, Kodanko and co-workers proposed two ruthenium(II)-photocaged ABI complexes **39** as controllable photoresponsive prodrugs.[116] Similar to the results described above, the biological activity of abiraterone is efficiently suppressed after being conjugated with the photosensitive ruthenium(II) complex. Irradiation of complex **39a** at 500 nm results in the photolysis of ABI within 2 min through ligand exchange with H_2O (Φ = 0.018), which subsequently interacts with CYP17A1. Further biological studies demonstrate that after irradiation of complex **39a**, the photoreleased ABI unit induces a sharp decrease in the viability of DU145 cells, whereas the ruthenium(II) byproducts remain non-cytotoxic.

6.2.3 Photorelease of NO and CO

NO and CO are important signalling molecules in physiological conditions and play crucial roles in biological processes at low concentrations, such as anti-inflammatory, blood pressure regulation and promoting cell growth.[117,118] Notably, high concentrations of NO and CO exhibit potential therapeutic effects. The design of photolabile transition metal nitrosyls and carbonyls complexes as photoNORM and photoCORM that deliver NO and CO, respectively, to the target tumours or tissues under UV or visible-red light excitation with controllable dosage control is of great interest.[119-121]

A phosphorescent ruthenium(II) complex (**40**) incorporated into carbon-doped titanium dioxide nanoparticles as cancer cell targetable NO-delivery nanoplatform has been proposed by Liu and co-workers.[122] The carbon-doped nanoparticles give the nanoplatform strong absorption in the NIR region, resulting in efficient NO and ROS release upon NIR light irradiation, with the NO-releasing quantum yield of 0.0174 ± 0.002 mol $Einstein^{-1}$. LSCM images reveal that the nanoplatform selectively targets the folic acid-positive cancer cell lines and mainly accumulates in the lysosome due to the presence of lysosome-targeting morpholine moiety. Mild NIR light irradiation allows the dual-targeted nanoplatform to exhibit strong photocytotoxicity against folate-receptor (FR) overexpressed HeLa cells compared to its non-targeting counterpart. In another study, a NIR light-activatable ruthenium(II) nitrosyl complex-based metallodrug ($[Ru^{II}(antpy)(bpy)(NO^{+})](PF_6)_3$ (antpy = 4'-(anthracene-9-yl)-2,2':6',2"-terpyridine) (**41**) has been developed by Maji and co-workers as a NO-mediated therapeutic compound.[123] NIR light irradiation of the complex leads to complete Ru–NO bond dissociation within 2 h with a rate constant of 9.4×10^{-3} min^{-1} and an obvious colour change of the solution, indicating the potential

ability of the complex to deliver NO in the photo-therapeutic window. In dark conditions, complex **41** and its photo-released ruthenium(II) byproducts display negligible cytotoxicity towards VCaP human prostate cancer cells. Upon irradiation, significant cell death is detected after incubation with complex **41**, with a reduction in IC_{50} value to 8.9 μM.

Tricarbonyl rhenium(I) polypyridine complexes $[Re(CO)_3(bpy)(X)]$ are the most broadly studied CO delivery platform. For example, a water-soluble carboxymethyl chitosan-modified rhenium(I) polypyridine complex $[Re(CO)_3(phen)(pyAl)](CF_3SO_3)$ (phen = 1,10-phenanthroline; pyAl = pyridine-4-carboxaldehyde) (**42**) has been synthesised by Mascharak and co-workers for photo-induced CO release.[124] UV irradiation triggers full dissociation of the complex in aqueous media, as evidenced by a clear change in the absorption spectra due to the liberation of CO molecules. Cellular studies show that the complex is rapidly internalised into different cancer cell lines and promotes significant CO-mediated human colorectal adenocarcinoma cells (HT-29) death after UV light irradiation.

In addition to rhenium(I) polypyridine complexes, photoactivatable ruthenium(II) complexes also exhibit excellent photo-induced CO release. Two ruthenium(II) dicarbonyl complexes containing an amide-modified bpy ligand (**43**) reveal efficient CO release properties, which have been proposed by Stephan and co-workers.[125] Exposure of the complexes to UV light results in a rapid monodecarbonylation. Co-localisation studies show that both complexes are localised in mitochondria after 30 min incubation and transferred to ER if the incubation time is extended to 4 h. Notably, after irradiation with UV light, an increase of apoptosis-mediated cell death is observed after cells are treated with complexes **43** as a result of the CO release.

7. Overview and future outlook

In this critical review, we have introduced some recent examples of TMCs for intracellular imaging, PDT and PACT. Strategic manipulation of the structural features of the TMCs can induce vast differences in their intracellular localisations. The long-lived triplet state lifetimes of TMCs make them efficient photosensitisers and their potent anticancer activity is present even under hypoxic conditions. Great lengths have been devoted to the design of NIR activatable TMCs by conjugation with organic dyes or utilisation of two-photon absorption techniques. The potential applications of organometallic TMCs as PACT reagents have also been explored as another means of therapeutic modality. Based on the recent studies on TMCs, we believe that the rational design of inorganic and organometallic TMCs with integrated diagnostic and therapeutic features will be of great interest for new biomedical applications. One area of interest is the improvement of cancer cell selectivity of traditional TMCs-based phototherapeutic agents to reduce their off-target cytotoxicity. The incorporation of TMCs with TME-responsive moieties could 1) enable the direct delivery of the TMCs; 2) enhance tumour accumulation; and 3) increase the efficiency of anticancer treatment. Many TMCs-based photoCORM and photoNORM have been studied, but these compounds are limited to *in cellulo* levels. Further biological studies are required before clinical use, such as possible interactions with biomolecules in intracellular settings, biostability, potential off-target cytotoxicity and *in vivo* efficiency.

Acknowledgements

We acknowledge the funding support from the Hong Kong Research Grants Council (Project No. CityU 11300017, CityU 11300318, CityU 11300019, CityU 11302820 and T42-103/16-N), and

"Laboratory for Synthetic Chemistry and Chemical Biology" under the Health@InnoHK Program launched by Innovation and Technology Commission, The Government of Hong Kong Special Administrative Region of the People's Republic of China. G.-X. X. acknowledges the receipt of a Postgraduate Studentship administered by City University of Hong Kong. E. C.-L. M. acknowledges the receipt of a Hong Kong Ph.D. Fellowship administered by the Research Grants Council of Hong Kong Special Administrative Region of the People's Republic of China.

1 A. Zamora, G. Vigueras, V. Rodríguez, M. D. Santana and J. Ruiz, Cyclometalated Iridium(III) Luminescent Complexes in Therapy and Phototherapy, *Coord. Chem. Rev.*, 2018, **360**, 34 – 76.

2 F. E. Poynton, S. A. Bright, S. Blasco, D. C. Williams, J. M. Kelly and T. Gunnlaugsson, The Development of Ruthenium(II) Polypyridyl Complexes and Conjugates for *in vitro* Cellular and *in vivo* Applications, *Chem. Soc. Rev.*, 2017, **46**, 7706 – 7756.

3 E. Villemin, Y. C. Ong, C. M. Thomas and G. Gasser, Polymer Encapsulation of Ruthenium Complexes for Biological and Medicinal Applications, *Nat. Rev. Chem.*, 2019, **3**, 261 – 282.

4 K. K.-W. Lo, Luminescent Rhenium(I) and Iridium(III) Polypyridine Complexes as Biological Probes, Imaging Reagents, and Photocytotoxic Agents, *Acc. Chem. Res.*, 2015, **48**, 2985 – 2995.

5 C. Imberti, P. Zhang, H. Huang and P. J. Sadler, New Designs for Phototherapeutic Transition Metal Complexes, *Angew. Chem. Int. Ed.*, 2020, **132**, 61 – 73.

6 M. R. Gill and J. A. Thomas, Ruthenium(II) Polypyridyl Complexes and DNA-from Structural Probes to Cellular Imaging and Therapeutics, *Chem. Soc. Rev.*, 2012, **41**, 3179 – 3192.

7 K. Y. Zhang, Q. Yu, H. Wei, S. Liu, Q. Zhao and W. Huang, Long-Lived Emissive Probes for Time-Resolved Photoluminescence Bioimaging and Biosensing, *Chem. Rev.*, 2018, **118**, 1770 – 1839.

8 R. Zhang and Y. Li, Responsive Metal Complex Probes for Time-Gated Luminescence Biosensing and Imaging, *Acc. Chem. Res.*, 2020, **53**, 7, 1316 – 1329.

9 Y. Chen, R. Guan, C. Zhang, J. Huang, L. Ji and H. Chao, Two-Photon Luminescent Metal Complexes for Bioimaging and Cancer Phototherapy, *Coord*. *Chem*. *Rev*., 2016, **310**, 16 – 40.

10 K. K.-W. Lo and S. P.-Y. Li, Utilization of the Photophysical and Photochemical Properties of Phosphorescent Transition Metal Complexes in the Development of Photofunctional Cellular Sensors, Imaging Reagents, and Cytotoxic Agents, *RSC Adv*., 2014, **4**, 10560 – 10585.

11 C.-N. Ko, G. Li, C.-H. Leung and D.-L. Ma, Dual Function Luminescent Transition Metal Complexes for Cancer Theranostics: The Combination of Diagnosis and Therapy, *Coord*. *Chem*. *Rev*., 2019, **381**, 79 – 103.

12 Y. Ma, H. Liang, Y. Zeng, H. Yang, C.-L. Ho, W. Xu, Q. Zhao, W. Huang and W.-Y. Wong, Phosphorescent Soft Salt for Ratiometric and Lifetime Imaging of Intracellular pH Variations, *Chem*. *Sci*., 2016, **7**, 3338 – 3346.

13 A. Kando, Y. Hisamatsu, H. Ohwada, T. Itoh, S. Moromizato, M. Kohno and S. Aoki, Photochemical Properties of Red-Emitting tris(cyclometalated) Iridium(III) Complexes Having Basic and Nitro Groups and Application to pH Sensing and Photoinduced Cell Death, *Inorg*. *Chem*., 2015, **54**, 5342 – 5357.

14 L. Murphy, A. Congreve, L.-O. Palsson and J. A. G. Williams, The Time Domain in Co-Stained Cell Imaging: Time-Resolved Emission Imaging Microscopy Using a Protonatable Luminescent Iridium Complex, *Chem*. *Commun*., 2010, **46**, 8743 – 8745.

15 H. Komatsu, K. Yoshihara, H. Yamada, Y. Kimura, A. Son, S.-I. Nishimoto and K. Tanabe, Ruthenium Complexes with Hydrophobic Ligands that are Key Factors for the Optical Imaging of Physiological Hypoxia, *Chem*. *Eur*. *J*., 2013, **19**, 1971 – 1977.

16 X. Zheng, X. Wang, H. Mao, W. Wu, B. Liu and X. Jiang, Hypoxia-Specific Ultrasensitive Detection of Tumours and Cancer Cells *in vivo*, *Nat*. *Commun*., 2015, **6**, 5834 – 5845.

17 L. H. Fischer, M. I. J. Stich, O. S. Wolfbeis, N. Tian, E. Holder and M. Schäferling, Red-and Green-Emitting Iridium(III) Complexes for a Dual Barometric and Temperature-Sensitive Pain, *Chem*. *Eur*. *J*., 2009, **15**, 10857 – 10863.

18 Y.-D. Zhuang, P.-Y. Chiang, C.-W. Wang and K.-T. Tan, Environment-Sensitive Fluorescent Turn-on Probes Targeting Hydrophobic Ligand-Binding Domains for Selective Protein Detection, *Angew*. *Chem*. *Int*. *Ed*., 2013, **52**, 8124 – 8128.

19 X. Liu, K. Li, L. Shi, H. Zhang, Y.-H Liu, H.-Y Wang, N. Wang and X.-Q. Yu, Purine-Based Ir(III) complexes for Sensing Viscosity of Endo-Plasmic Reticulum with Fluorescence Lifetime Imaging Microscopy, *Chem*. *Commun*., 2021, **18**, 2265 – 2268.

20 F. Liu, J. Wen, S.-S. Chen and S. Sun, A Luminescent Bimetallic Iridium(III) Complex for Ratiometric Tracking Intracellular Viscosity, *Chem*. *Commun*., 2018, **54**, 1371 – 1374.

21 K. D. Mjos and C. Orvig, Metallodrugs in Medicinal Inorganic Chemistry, *Chem*. *Rev*., 2014, **114**, 4540 – 4563.

22 S. Monro, K. L. Colon, H. Yin, J. Roque, P. Konda, S. Gujar, R. P. Thummel, L. Lilge, C. G. Cameron and S. A. McFarland, Transition Metal Complexes and Photodynamic Therapy from a Tumor-Centered Approach: Challenges, Opportunities, and Highlights from the Development of TLD1433, *Chem*. *Rev*., 2019, **119**, 797 – 828.

23 K. K.-W. Lo and K. Y. Zhang, Iridium(III) Complexes as Therapeutic and Bioimaging Reagents for Cellular Applications, *RSC Adv*., 2012, **2**, 12069 – 12083.

24 K. K.-W. Lo, A. W.-T. Choi and W.-H. Law, Applications of Luminescent Inorganic and Organometallic Transition Metal Complexes as Biomolecular and Cellular Probes, *Dalton Trans*., 2012, **41**, 6021 – 6027.

25 J. D. Knoll, B. A. Albani and C. Turro, New Ru(II) Complexes for Dual Photoreactivity: Ligand Exchange and $^1O_2$ Generation, *Acc*. *Chem*. *Res*., 2015, **48**, 2280 – 2287.

26 J. Shum, P. K.-K. Leung and K. K.-W. Lo, Luminescent Ruthenium(II) Polypyridine Complexes for a Wide Variety of Biomolecular and Cellular Applications, *Inorg*. *Chem*., 2019, **58**, 2231 – 2247.

27 Z. Huang and J. J. Wilson, Therapeutic and Diagnostic Applications of Multimetallic Rhenium(I) Tricarbonyl Complexes, *Eur*. *J*. *Inorg*. *Chem*., 2021, **14**, 1312 – 1324.

28 P.-Y. Ho, C.-L. Ho and W.-Y. Wong, Recent Advances of Iridium(III) Metallophosphors for Health-Related Applications, *Coord*. *Chem*. *Rev*., 2020, **413**, 213267 – 213304.

29 H. Jin, X. Jiang, Z. Sun and R. Gui, Phosphorescence-based ratiometric probes: Design, preparation and applications in sensing, imaging and biomedicine therapy, *Coord*. *Chem*. *Rev*., 2021, **431**, 213694 – 213732.

30 C.-X. Yin, K.-M. Xiong, F.-J. Huo, J. C. Salamanca and R. M. Strongin, Fluorescent Probes with Multiple Binding Sites for the Discrimination of Cys, Hcy, and GSH, *Angew*. *Chem*. *Int*. *Ed*., 2017, **56**, 13188 – 1319.

31 D. W. Bak, T. J. Bechtel, J. A. Falco and E. Weerapana, Cysteine Reactivity Across the Subcellular Universe, *Curr*. *Opin*. *Chem*. *Biol*., 2019, **48**, 96 – 105.

32 J. Selhub, Homocysteine Metabolism, *Annu*. *Rev*. *Nutr*., 1999, **19**, 217 – 246.

33 N. Ballatori, S. M. Krance, S. Notenboom, S. Shi, K. Tieu and C. L. Hammond, Glutathione Dysregulation and the Etiology and Progression of Human Diseases, *Biol. Chem*., 2009, **390**, 191 – 214.

34 G. Wu, Y.-Z. Fang, S. Yang, J. R. Lupton and N. D. Turner, Glutathione Metabolism and Its Implications for Health, *J. Nutr*., 2004, **134**, 489 – 492.

35 V. S. Lin, W. Chen, M. Xian and C. J. Chang, Chemical Probes for Molecular Imaging and Detection of Hydrogen Sulfide and Reactive Sulfur Species in Biological Systems, *Chem. Soc. Rev*., 2015, **44**, 4596 – 4618.

36 S. P.-Y. Li, J. Shum and K. K.-W. Lo, Iridium(III) Polypyridine Complexes with a Disulfide Linker as Biological Sensors and Cytotoxic Agents, *Dalton Trans*., 2019, **48**, 9692 – 9702.

37 C. Liu, J. Liu, W. Zhang, Y.-L. Wang, Q. Liu, B. Song, J. Yuan and R. Zhang, Two Birds with One Stone" Ruthenium(II) Complex Probe for Biothiols Discrimination and Detection *in vitro* and *in vivo*, *Adv. Sci*., 2020, **7**, 2000458 – 2000467.

38 T. F. Brewer and C. J. Chang, An Aza-Cope Reactivity-Based Fluorescent Probe for Imaging Formaldehyde in Living Cells, *J. Am. Chem. Soc*., 2015, **137**, 10886 – 10889.

39 Y. Tang, X. Kong, Z.-R. Liu, A. Xu and W. Lin, Lysosome-Targeted Turn-on Fluorescent Probe for Endogenous Formaldehyde in Living Cells, *Anal. Chem*., 2016, **88**, 9359 – 9363.

40 C. Liu, R. Zhang, W. Zhang, J. Liu, Y.-L. Wang, Z. Du, B. Song, Z. P. Xu and J. Yuan, Dual-key-and-lock" Ruthenium Complex Probe for Lysosomal Formaldehyde in Cancer Cells and Tumors, *J. Am. Chem. Soc*., 2019, **141**, 8462 – 8472.

41 C. Szabó, H. Ischiropoulos and R. Radi, Peroxynitrite: Biochemistry, Pathophysiology and Development of Therapeutics, *Nat*. *Rev*. *Drug Discovery*, 2007, **6**, 662 – 680.

42 Z. Chen, X. Meng, L. Zou, M. Zhao, S. Liu, P. Tao, J. Jiang and Q. Zhao, A Dual-Emissive Phosphorescent Polymeric Probe for Exploring Drug-Induced Liver Injury via Imaging of Peroxynitrite Elevation *in vivo*, *ACS Appl*. *Mater*. *Interfaces*, 2020, **12**, 12383 – 12394.

43 D. Wu, L. Chen, Q. Xu, X. Chen and J. Yoon, Design Principles, Sensing Mechanisms, and Applications of Highly Specific Fluorescent Probes for HOCl/OCl^-, *Acc*. *Chem*. *Res*., 2019, **52**, 2158 – 2168.

44 Y. Dai, Z. Zhan, L. Chai, L. Zhang, Q. Guo, K. Zhang and Y. Lv, A Two-Photon Excited Near-Infrared Iridium(III) Complex for Multi-Signal Detection and Multimodal Imaging of Hypochlorite, *Anal*. *Chem*., 2021, **93**, 4628 – 4634.

45 T. Rosse, R. Olivier, L. Monney, M. Rager, S. Conus, I. Fellay, B. Jansen and C. Borner, Bcl-2 Prolongs Cell Survival after BaxInduced Release of Cytochrome c, *Nature*, 1998, **391**, 496 – 499.

46 A. G. Porter and R. U. Jänicke, Emerging Roles of Caspase-3 in Apoptosis, *Cell Death Differ*., 1999, **6**, 99 – 104.

47 Q. Wu, K. Y. Zhang, P. Dai, H. Zhu, Y. Wang, L. Song, L. Wang, S. Liu, Q. Zhao and W. Huang, Labeling after Recognition" Affording an FRET-Based Luminescent Probe for Detecting and Imaging Caspase-3 via Photoluminescence Lifetime Imaging, *J*. *Am*. *Chem*. *Soc*., 2020, **142**, 1057 – 1064.

48 A. L. Harris, Hypoxia-a Key Regulatory Factor in Tumour Growth, *Nat*. *Rev*. *Cancer*, 2002, **2**, 38 – 47.

49 D. Jamieson, B. Chance, E. Cadenas and A. Boveris, The Relation of Free Radical Production to Hyperoxia, *Annu*. *Rev*. *Physiol*., 1986, **48**, 703 – 719.

50 K. Y. Zhang, P. Gao, G. Sun, T. Zhang, X. Li, S. Liu, Q. Zhao, K. K.-W. Lo and W. Huang, Dual-Phosphorescent Iridium(III) Complexes Extending Oxygen Sensing from Hypoxia to Hyperoxia, *J*. *Am*. *Chem*. *Soc*., 2018, **140**, 7827 – 7834.

51 M. K. Kuimova, S. W. Botchway, A. W. Parker, M. Balaz, H. A. Collins, H. L. Anderson, K. Suhling and P. R. Ogilby, Imaging Intracellular Viscosity of a Single Cell during Photoinduced Cell Death, *Nat*. *Chem*., 2009, **1**, 69 – 73.

52 L. Hao, Z.-W. Li, D.-Y. Zhang, L. He, W. Liu, J. Yang, C.-P. Tan, L.-N. Ji and Z.-W. Mao, Monitoring Mitochondrial Viscosity with Anticancer Phosphorescent Ir(III) Complexes via Two-Photon Lifetime Imaging, *Chem*. *Sci*., 2019, **10**, 1285 – 1293.

53 S. J. Singer and G. L. Nicolson, The Fluid Mosaic Model of the Structure of Cell Membranes, *Science*, 1972, **175**, 720 – 731.

54 K. Y. Zhang, T. Zhang, H. Wei, Q. Wu, S. Liu, Q. Zhao and W. Huang, Phosphorescent Iridium(III) Complexes Capable of Imaging and Distinguishing between Exogenous and Endogenous Analytes in Living Cells, *Chem*. *Sci*., 2018, **9**, 7236 – 7240.

55 K. Y. Zhang, L. Song, T. Gu, H. Wang, C. Yang, H. Zhou, P. Gao, S. Liu and Q. Zhao, Cell-Membrane Staining Properties and Photocytotoxicity of a Ruthenium(II) Photosensitizer, *Eur*. *J*. *Inorg*. *Chem*., 2020, **42**, 3996 – 4001.

56 J. Nunnari and A. Suomalainen, Mitochondria: in Sickness and in Health, *Cell*, 2012, **148**, 1145 – 1159.

57 L. C.-C. Lee, H. M.-H. Cheung, H.-W. Liu and K. K.-W. Lo, Exploitation of Environment-Sensitive Luminophores in the Design of Sydnone-Based Bioorthogonal Imaging Reagents, *Chem*. *Eur*. *J*., 2018, **24**, 14064 – 14068.

58 C. S. Burke, A. Byrne and T. E. Keyes, Highly Selective Mitochondrial Targeting by a Ruthenium(II) Peptide Conjugate: Imaging and Photoinduced Damage of Mitochondrial DNA, *Angew*. *Chem*. *Int*. *Ed*., 2018, **57**, 12420 – 12424.

59 P. Saftig and J. Klumperman, Lysosome Biogenesis and Lysosomal Membrane Proteins: Trafficking Meets Function, *Nat*. *Rev*. *Mol*. *Cell*. *Biol*., 2009, **10**, 623 – 635.

60 A. Ballabio and J. S. Bonifacino, Lysosomes as Dynamic Regulators of Cell and Organismal Homeostasis, *Nat*. *Rev*. *Mol*. *Cell Biol*., 2020, **21**, 101 – 118.

61 J. Shum, P.-Z. Zhang, L. C.-C. Lee and K. K.-W. Lo, Bioorthogonal Phosphorogenic Rhenium(I) Polypyridine Sydnone Complexes for Specific Lysosome Labeling, *ChemPlusChem*, 2020, **85**, 1374 – 1378.

62 C. Jin, G. Li, X. Wu, J. Liu, W. Wu, Y. Chen, T. Sasaki, H. Chao and Y. Zhang, Robust Packing of a Self-Assembling Iridium Complex via Endocytic Trafficking for Long-Term Lysosome Tracking, *Angew*. *Chem*. *Int*. *Ed*., 2021, **60**, 7597 – 7601.

63 D. Görlich and U. Kutay, Transport between the Cell Nucleus and the Cytoplasm, *Annu*. *Rev*. *Cell Dev*. *Biol*., 1999, **15**, 607 – 660.

64 A. H. Day, M. H. Übler, H. L. Best, E. Lloyd-Evans, R. J. Mart, I. A. Fallis, R. K. Allemann, E. A. H. Al-Wattar, N. I. Keymer, N. J. Buurma and S. J. A. Pope, Targeted Cell Imaging Properties of a Deep Red Luminescent Iridium(III) Complex Conjugated with a c-Myc Signal Peptide, *Chem*. *Sci*., 2020, **11**, 1599 – 1606.

65 L. Mascheroni, V. Francia, B. Rossotti, E. Ranucci, P. Ferruti, D. Maggioni and A. Salvati, Light-Triggered Trafficking to the Cell Nucleus of a Cationic Polyamidoamine Functionalized with Ruthenium Complexes, *ACS Appl*. *Mater*. *Interfaces*, 2020, **12**, 34576 – 34587.

66 H. K. Saeed, S. Sreedharan, P. J. Jarman, S. A. Archer, S. D. Fairbanks, S. P. Foxon, A. J. Auty, D. Chekulaev, T. Keane, A. J. H. M. Meijer, J. A. Weinstein, C. G. W. Smythe, J. B. de la Serna and J. A. Thomas, Making the Right Link to Theranostics: The Photophysical and Biological Properties of Dinuclear Ru^{II}-Re^{I} dppz Complexes Depend on Their Tether, *J*. *Am*. *Chem*. *Soc*., 2020, **142**, 1101 – 1111.

67 A. P. Castano, P. Mroz and M. R. Hamblin, Photodynamic Therapy and Anti-Tumour Immunity, *Nat. Rev*. *Cancer*, 2006, **6**, 535 – 545.

68 M. Ethirajan, Y. Chen, P. Joshi and R. K. Pandey, The Role of Porphyrin Chemistry in Tumor Imaging and Photodynamic Therapy, *Chem*. *Soc*. *Rev*., 2011, **40**, 340 – 362.

69 T. Joshi, V. Pierroz, C. Mari, L. Gemperle, S. Ferrari and G. Gasser, A Bis(dipyridophenazine)(2-(2-pyridyl)pyrimidine-4-carboxylic acid)ruthenium(II) Complex with Anticancer Action upon Photodeprotection, *Angew*. *Chem*. *Int*. *Ed*., 2014, **126**, 3004 – 3007.

70 K. K.-W. Lo, Molecular Design of Bioorthogonal Probes and Imaging Reagents Derived from Photofunctional Transition Metal Complexes, *Acc*. *Chem*. *Res*., 2020, **53**, 32 – 44.

71 R. K Jain, Normalization of Tumor Vasculature: an Emerging Concept in Antiangiogenic Therapy, *Science*, 2005, **307**, 58 – 62.

72 M. W Dewhirst, Y. Cao and B. Moeller, Cycling Hypoxia and Free Radicals Regulate Angiogenesis and Radiotherapy Response, *Nat*. *Rev*. *Cancer*, 2008, **8**, 425 – 437.

73 B. Doix, E. Bastien, A. Diman, A. Decottignies, O. Feron and B. Elias, Exploring the Phototoxicity of Hypoxic Active Iridium(III)-based Sensitizers in 3D Tumor Spheroids, *J*. *Am*. *Chem*. *Soc*., 2019, **141**, 18486 – 18491.

74 F. J. Ballester, E. Ortega, D. Bautista, M. D. Santana and J. Ruiz, Ru(II) Photosensitizers Competent for Hypoxic Cancers via Green Light Activation, *Chem*. *Commun*., 2020, **56**, 10301 – 10304

75 Z. Lv, H. Wei, Q. Li, X. Su, S. Liu, K. Y. Zhang, W. Lv, Q. Zhao, X. Li and W. Huang, Achieving Efficient Photodynamic Therapy under both Normoxia and Hypoxia Using Cyclometalated Ru(II) Photosensitizer Through type I Photochemical Process, *Chem*. *Sci*., 2018, **9**, 502 – 512.

76 J. Ge, M. Lan, B. Zhou, W. Liu, L. Guo, H. Wang, Q. Jia, G. Niu, X. Huang, H. Zhou, X. Meng, P. Wang, C.-S. Lee, W. Zhang and X. Han, A Graphene Quantum Dot Photodynamic Therapy Agent with High Singlet Oxygen Generation, *Nat*. *Commun*., 2014, **5**, 4596 – 4603.

77 L. C.-C. Lee, K.-K. Leung and K. K.-W. Lo, Recent Development of Luminescent Rhenium(I) Tricarbonyl Polypyridine Complexes as Cellular Imaging Reagents, Anticancer Drugs, and Antibacterial Agents, *Dalton Trans*., 2017, **46**, 16357 – 16380.

78 J. Liu, C. Zhang, T. W. Rees, L. Ke, L. Ji and H. Chao, Harnessing Ruthenium(II) as Photodynamic Agents: Encouraging Advances in Cancer Therapy, *Coord*. *Chem*. *Rev*., 2018, **363**, 17 – 28.

79 P. K.-K. Leung and K. K.-W. Lo, Modulation of Emission and Singlet Oxygen Photosensitisation in Live Cells Utilising Bioorthogonal Phosphorogenic Probes and Protein Tag Technology, *Chem*. *Commun*., 2020, **56**, 6074 – 6077.

80 B. Liu, S. Monro, Z. Li, M. A. Jabed, D. Ramirez, C. G. Cameron, K. Colón, J. Roque III, S. Kilina, J. Tian, S. A. McFarland and W. Sun, New Class of Homoleptic and Heteroleptic Bis (terpyridine) Iridium(III) Complexes with Strong Photodynamic Therapy Effects, *ACS Appl*. *Bio. Mater*., 2019, **2**, 2964 – 2977.

81 P. Zhang, H. Huang, S. Banerjee, G. J. Clarkson, C. Ge, C. Imberti and P. J. Sadler, Nucleus-Targeted Organoiridium-Albumin Conjugate for Photodynamic Cancer Therapy, *Angew*. *Chem*. *Int*. *Ed*., 2019, **58**, 2350 – 2354.

82 L. C.-C. Lee, A. W.-Y. Tsang, H.-W. Liu and K. K.-W. Lo, Photofunctional Cyclometalated Iridium (III) Polypyridine Complexes Bearing a Perfluorobiphenyl Moiety for Bioconjugation, Bioimaging, and Phototherapeutic Applications, *Inorg*. *Chem*., 2020, **59**, 14796 – 14806.

83 Y. Shen, A. J. Shuhendler, D. Ye, J.-J. Xua and H.-Y. Chen, Two-Photon Excitation Nanoparticles for Photodynamic Therapy, *Chem*. *Soc*. *Rev*., 2016, **45**, 6725 – 6741.

84 L. K. McKenzie, H. E. Bryant and J. A. Weinstein, Transition Metal Complexes as Photosensitisers in One-and Two-Photon Photodynamic Therapy, *Coord*. *Chem*. *Rev*., 2019, **379**, 2 – 29.

85 Z. Zhou, J. Liu, T. W. Rees, H. Wang, X. Lic, H. Chao and P. J. Stang, Heterometallic Ru–Pt Metallacycle for Two-Photon Photodynamic Therapy, *Proc*. *Natl*. *Acad*. *Sci*. *USA*, 2018, **115**, 5664 – 5669.

86 J. Karges, S. Kuang, F. Maschietto, O. Blacque, I. Ciofini, H. Chao and G. Gasser, Rationally Designed Ruthenium Complexes for 1- and 2-Photon Photodynamic Therapy, *Nat*. *Commun*., 2020, **11**, 3262 – 3274.

87 P. Miłosz, H. A. Collins, R. G. Denning and H. L. Anderson, Two-Photon Absorption and the Design of Two-Photon Dyes, *Angew*. *Chem*. *Int*. *Ed*., 2009, **48**, 3244 – 3266.

88 J. Liu, C. Jin, B. Yuan, X. Liu, Y. Chen, L. Jia and H. Chao, Selectively Lighting Up Two-Photon Photodynamic Activity in Mitochondria with AIE-Active Iridium(III) Complexes, *Chem*. *Commun*., 2017, **53**, 2052 – 2055.

89 I. Lim, A. Vian, H. L. van de Wouw, R. A. Day, C. Gomez, Y. Liu, A. L. R. O. Campàs and E. M. Sletten, Fluorous Soluble Cyanine Dyes for Visualizing Perfluorocarbons in Living Systems, *J*. *Am*. *Chem*. *Soc*., 2020, **142**, 16072 – 16081.

90 W. Guo, Q. Wang and J. Zhu, Selective 1, 2-Aminoisothiocyanation of 1, 3-Dienes Under Visible-Light Photoredox Catalysis, *Angew*. *Chem*. *Int*. *Ed*., 2021, **60**, 4085 – 4089.

91 Q. Yang, H. Jin, Y. Gao, J. Lin, H. Yang and S. Yang, Photostable Iridium(III)-Cyanine Complex Nanoparticles for Photoacoustic Imaging Guided Near-Infrared Photodynamic Therapy *in vivo*, *ACS Appl*. *Mater*. *Interfaces*, 2019, **11**, 15417 – 15425.

92 G. Gupta, A. Das, S. Panja, J. Y. Ryu, J. Lee, N. Mandal and C. Y. Lee, Self-Assembly of Novel Thiophene-Based BODIPY RuII Rectangles: Potential Antiproliferative Agents Selective Against Cancer Cells, *Chem*. *Eur*. *J*., 2017, **23**, 17199 – 17203.

93 R. P. Paitandi, S. Mukhopadhyay, R. S. Singh, V. Sharma, S. M. Mobin and D. S. Pandey, Anticancer Activity of Iridium(III) Complexes based on a Pyrazole-Appended Quinoline-based BODIPY. *Inorg*. *Chem*., 2017, **56**, 12232 – 12247.

94 P. Majumdar, X. Yuan, S. Li, B. L. Guennic, J. Ma, C. Zhang, D. Jacqueminde and J. Zhao, Cyclometalated Ir(III) Complexes with Styryl-BODIPY Ligands Showing Near IR Absorption/Emission: Preparation, Study of Photophysical Properties and Application as Photodynamic/Luminescence Imaging Materials, *J*. *Mater*. *Chem*. *B*, 2014, **2**, 2838 – 2854.

95 L. Qiao, J. Liu, Y. Han, F. Wei, X. Liao, C. Zhang, L. Xie, L. Jia and H. Chao, Rational Design of a Lysosome-Targeting and Near-Infrared Absorbing Ru(II)-BODIPY Conjugate for Photodynamic Therapy, *Chem*. *Commun*., 2021, **57**, 1790 – 1793.

96 R. E. Mahnken, M. A. Billadeau, E. P. Nikonowicz and H. Morrison, Development of Photo cis-Platinum Reagents. Reaction of cis-Dichlorobis (1, 10-phenanthroline) Rhodium(III) with Calf Thymus DNA, Nucleotides and Nucleosides, *J*. *Am*. *Chem*. *Soc*., 1992, **114**, 9253 – 9265.

97 N. A. Kratochwil, P. J. Bednarski, H. Mrozek, A. Vogler and J. K. Nagle, Photolysis of an Iodoplatinum (IV) Diamine Complex to Cytotoxic Species by Visible Light, *Anti-cancer Drug Des*., 1996, **11**, 155 – 171.

98 N. J. Farrer, J. A. Woods, L. Salassa, Y. Zhao, K. S. Robinson, G. Clarkson, F. S. Mackay and P. J. Sadler, A Potent Trans-Diimine Platinum Anticancer Complex Photoactivated by Visible Light, *Angew*. *Chem*. *Int*. *Ed*., 2010, **49**, 8905 – 8908.

99 H. Shi, C. Imberti and P. J. Sadler, Diazido Platinum(IV) Complexes for Photoactivated Anticancer Chemotherapy, *Inorg. Chem. Front.*, 2019, **6**, 1623 – 1638.

100 R. E. Goldbach, I. Rodriguez-Garcia, J. H. van Lenthe, M. A. Siegler and S. Bonnet, *N*-Acetylmethionine and Biotin as Photocleavable Protective Groups for Ruthenium Polypyridyl Complexes, *Chem. Eur. J.*, 2011, **17**, 9924 – 9929.

101 L. N. Lameijer, D. Ernst, S. L. Hopkins, M. S. Meijer, S. H. C. Askes, S. E. L. Dévédec and S. Bonnet, A Red-Light-Activated Ruthenium-Caged NAMPT Inhibitor Remains Phototoxic in Hypoxic Cancer Cells, *Angew. Chem. Int. Ed.*, 2017, **56**, 11549 – 11711.

102 R. N. Garner, J. C. Gallucci, K. R. Dunbar and C. Turro, $[Ru(bpy)_2(5\text{-cyanouracil})_2]^{2+}$ as a Potential Light-Activated Dual-Action Therapeutic Agent, *Inorg. Chem.*, 2011, **50**, 9213 – 9215.

103 C. F. Works and P. C. Ford, Photoreactivity of the Ruthenium Nitrosyl Complex, Ru (salen)(Cl)(NO). Solvent Effects on the Back Reaction of NO with the Lewis Acid Ru^{III} (salen)(Cl), *J. Am. Chem. Soc.*, 2000, **122**, 7592 – 7593.

104 P. C. Ford, Metal Complex Strategies for Photo-Uncaging the Small Molecule Bioregulators Nitric Oxide and Carbon Monoxide, *Coord. Chem. Rev.*, 2018, **376**, 548 – 564.

105 P. J. Bednarski, K. Korpis, A. F. Westendorf, S. Perfahl and R. Grünert, Effects of Light-Activated Diazido-Pt^{IV} Complexes on Cancer Cells *in vitro*, *Philos. Trans. R. Soc. A*, 2013, **371**, 20120118 – 20120132.

106 F. S. Mackay, J. A. Woods, P. Heringova, J. Kasparkova, A. M. Pizarro, S. A. Moggach, S. Parsons, V. Brabec and P. J. Sadler, A Potent Cytotoxic Photoactivated Platinum Complex, *Proc*. *Natl*. *Acad*. *Sci*. *USA*, 2007, **104**, 20743 – 20748.

107 A. Garai, I. Pant, S. Banerjee, B. Banik, P. Kondaiah and A. R. Chakravarty, Photorelease and Cellular Delivery of Mitocurcumin from its Cytotoxic Cobalt(III) Complex in Visible Light, *Inorg*. *Chem*., 2016, **55**, 6027 – 6035.

108 N. A. Smith and P. J. Sadler, Photoactivatable Metal Complexes: from Theory to Applications in Biotechnology and Medicine, *Philos*. *Trans*. *R*. *Soc*. *A*, 2013, **371**, 1 – 12.

109 V. Novohradsky, J. Pracharova, J. Kasparkova, C. Imberti, H. E. Bridgewater, P. J. Sadler and V. Brabec, Induction of Immunogenic Cell Death in Cancer Cells by a Photoactivated Platinum (IV) Prodrug, *Inorg*. *Chem*. *Front*., 2020, **7**, 4150 – 4159.

110 A. M.-H. Yip and K. K.-W. Lo, Luminescent Rhenium(I), Ruthenium(II), and Iridium(III) Polypyridine Complexes Containing a Poly(ethylene glycol) Pendant or Bioorthogonal Reaction Group as Biological Probes and Photocytotoxic Agents, *Coord*. *Chem*. *Rev*., 2018, **361**, 138 – 163.

111 K. K.-S. Tso, K.-K. Leung, H.-W. Liu and K. K.-W. Lo, Photoactivatable Cytotoxic Agents Derived from Mitochondria-Targeting Luminescent Iridium(III) poly (ethylene glycol) Complexes Modified with a Nitrobenzyl Linkage, *Chem*. *Commun*., 2016, **52**, 4557 – 4560.

112 K. Mitra, C. E. Lyons and M. C. T. Hartman, A Platinum(II) Complex of Heptamethine Cyanine for Photoenhanced Cytotoxicity and Cellular Imaging in Near-IR Light, *Angew*. *Chem*. *Int*. *Ed*., 2018, **57**, 10263 – 10267.

113 W. Sun, S. Li, B. Häupler, J. Liu, S. Jin, W. Steffen, U. S. Schubert, H.-J. Butt, X.-J. Liang and S. Wu, An Amphiphilic Ruthenium Polymetallodrug for Combined Photodynamic Therapy and Photochemotherapy *in vivo*, *Adv*. *Mater*., 2017, **29**, 1603702 – 1603707.

114 N. P. Toupin, S. Nadella, S. J. Steinke, C. Turro and J. J. Kodanko, Dual-Action Ru(II) Complexes with Bulky π-Expansive Ligands: Phototoxicity without DNA Intercalation, *Inorg*. *Chem*., 2020, **59**, 3919 – 3933.

115 V. H. S. van Rixel, V. Ramu, A. B. Auyeung, N. Beztsinna, D. Y. Leger, L. N. Lameijer, S. T. Hilt, S. E. L. Dévédec, T. Yildiz, T. Betancourt, M. B. Gildner, T. W. Hudnall, V. Sol, B. Liagre, A. Kornienko and S. Bonnet, Photo-Uncaging of a Microtubule-Targeted Rigidin Analogue in Hypoxic Cancer Cells and in a Xenograft Mouse Model, *J*. *Am*. *Chem*. *Soc*., 2019, **141**, 18444 – 18454.

116 A. Li, R. Yadav, J. K. White, M. K. Herroon, B. P. Callahan, I. Podgorski, C. Turro, E. E. Scott and J. J. Kodanko, Illuminating Cytochrome P450 Binding: Ru(II)-Caged Inhibitors of CYP17A1, *Chem*. *Commun*., 2017, **53**, 3673 – 3676.

117 D. Crespy, K. Landfester, U. S. Schubert and A. Schiller, Potential Photoactivated Metallopharmaceuticals: from Active Molecules to Supported Drugs, *Chem*. *Commun*., 2010, **46**, 6651 – 6662.

118 A. W. Carpenter and M. H. Schoenfisch, Nitric Oxide Release: Part II. Therapeutic Applications, *Chem*. *Soc*. *Rev*., 2012, **41**, 3742 – 3752.

119 A. E. Pierri, A. Pallaoro, G. Wu and P. C. Ford, A Luminescent and Biocompatible photoCORM, *J*. *Am*. *Chem*. *Soc*., 2012, **134**, 18197 – 18200.

120 C. Bischof, T. Joshi, A. Dimri, L. Spiccia and U. Schatzschneider, Synthesis, Spectroscopic Properties, and Photoinduced CO-Release Studies of Functionalized Ruthenium(II) Polypyridyl Complexes: Versatile Building Blocks for Development of CORM-Peptide Nucleic Acid Bioconjugates, *Inorg*. *Chem*., 2013, **52**, 9297 – 9308.

121 I. Chakraborty, J. Jimenez, W. M. C. Sameera, M. Kato and P. K. Mascharak, Luminescent Re(I) Carbonyl Complexes as Trackable PhotoCORMs for CO Delivery to Cellular Targets, *Inorg*. *Chem*., 2017, **56**, 2863 – 2873.

122 H.-J. Xiang, Q. Deng, L. An, M. Guo, S.-P. Yang and J.-G. Liu, Tumor Cell Specific and Lysosome-Targeted Delivery of Nitric Oxide for Enhanced Photodynamic Therapy Triggered by 808 nm Near-Infrared Light, *Chem*. *Commun*., 2016, **52**, 148 – 151.

123 B. Giri, T. Saini, S. Kumbhakar, K. Selvan K, A. Muley, A. Misra and S. Maji, Near-IR Light-Induced Photorelease of Nitric Oxide (NO) on Ruthenium Nitrosyl Complexes: Formation, Reactivity, and Biological Effects, *Dalton Trans*., 2020, **49**,10772 – 10785.

124 I. Chakraborty, J. Jimenez and P. K. Mascharak, CO-Induced Apoptotic Death of Colorectal Cancer Cells by a Luminescent PhotoCORM Grafted on Biocompatible Carboxymethyl Chitosan, *Chem*. *Commun*., 2017, **53**, 5519 – 5522.

125 S. Geri, T. Krunclova, O. Janouskova, J. Panek, M. Hruby, D. Hernández-Valdés, B. Probst, R. A. Alberto, C. Mamat, M. Kubeil and H. Stephan, Light-Activated Carbon Monoxide Prodrugs Based on Bipyridyl Dicarbonyl Ruthenium(II) Complexes, *Chem*. *Eur*. *J*., 2020, **26**, 10992 – 11006.

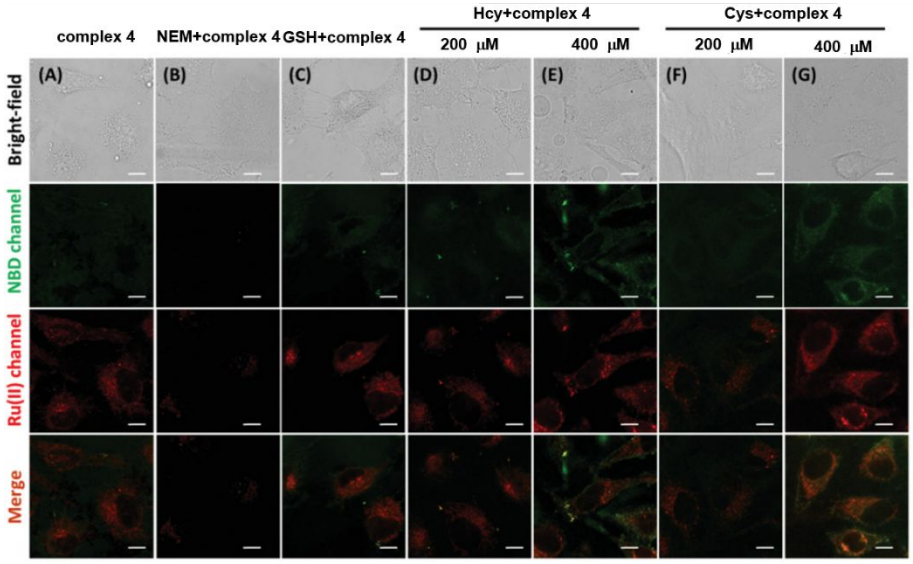

Fig. 1 (a) LSCM images of HeLa cells incubated with complex **4** (50 μM, 5 h). (b) LSCM images of HeLa cells pretreated with *N*-ethylmaleimide (NEM, 100 μM, 2 h), followed by staining with complex **4** (50 μM, 5 h). (c – g) LSCM images of HeLa cells pretreated with GSH (200 μM), Hcy (200 μM), Hcy(400 μM), Cys (200 μM) and Cys (400 μM), respectively, for 2 h, followed by staining with complex **4** (50 μM, 5 h). Scale bar = 10 μm. Reproduced with permission from ref. 37.

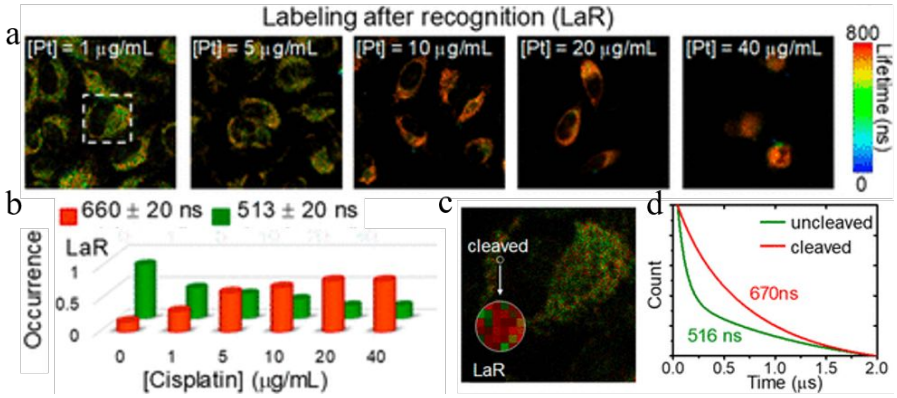

Fig. 2 (a) PLIM images of HeLa cells stimulated with cisplatin at different concentrations for 4 h through labelling after recognition approach. (b) Relative occurrence of long-lived and short-lived signals during lifetime imaging. (c) Enlarged view of the marked area in (a) and photoluminescence decay curves of the circled area. Scale bar = 20 μm. Reproduced with permission from ref. 47.

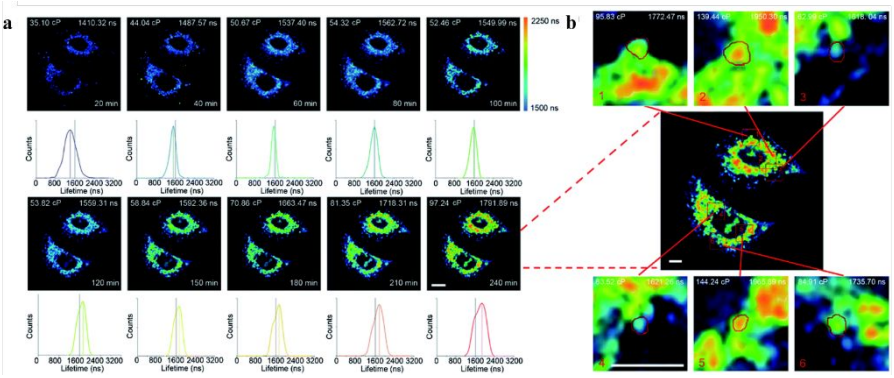

Fig. 3 (a) Two-photon PLIM images of A549 cells incubated with complex **10f** (20 μM) subjected to imaging at different time intervals. (b) Two-photon PLIM images of A549 cells incubated with complex **10f** (20 μM, 4 h). The enlarged images are from the red boxes. The lifetime and viscosity are calculated from the spots in the red circle. Reproduced with permission from ref. 52.

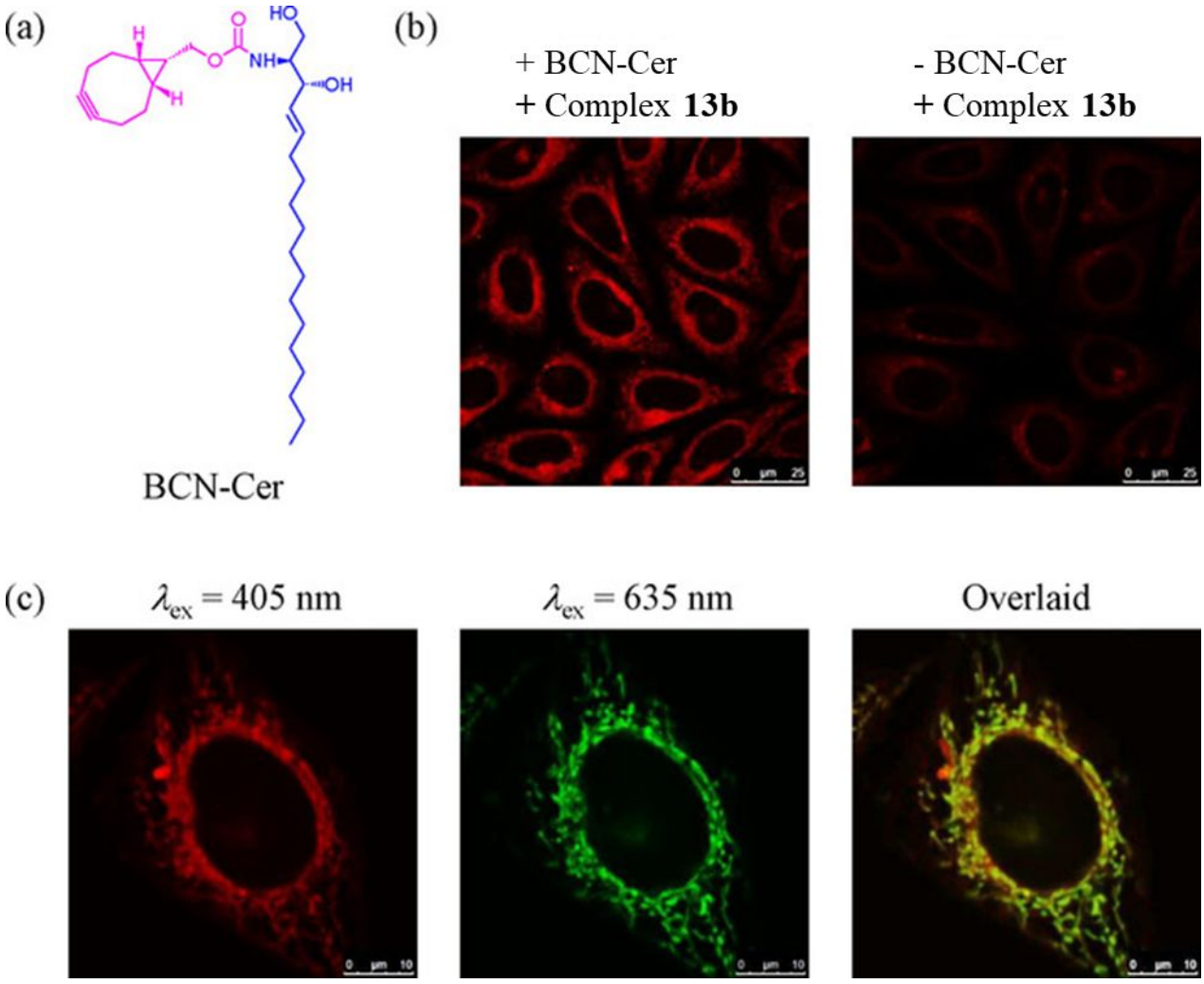

Fig. 4 (a) Structure of BCN-Cer. (b) LSCM images of live HeLa cells incubated with complex **13b** (5 μM, 4 h) with (left) or without (right) pretreatment with BCN-Cer (125 μM, 1 h) at 37 °C. (c) LSCM images of live HeLa cells pretreated with BCN-Cer (125 μM, 1 h) and incubated with complex **13b** (5 μM, 4 h, λ_{ex}=405 nm) and MitoTracker® Deep Red FM (100 nM, 20 min, λ_{ex}=635 nm) at 37 °C (Pearson's correlation coefficient = 0.93). Reproduced with permission from ref. 57.

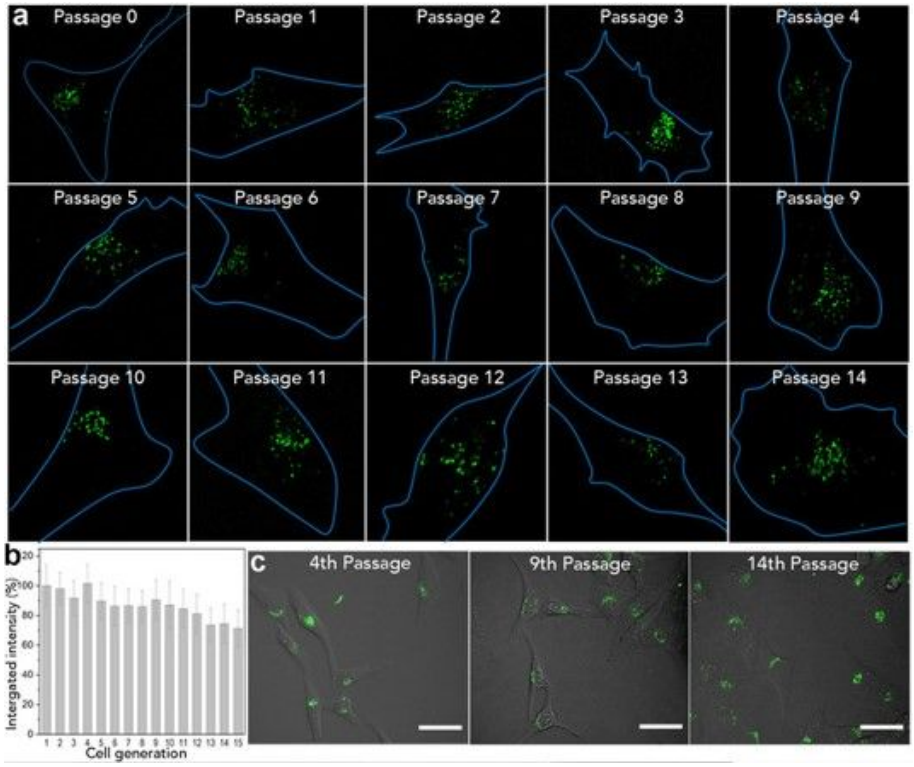

Fig. 5 (a) LSCM images of a HeLa cell at passage 0 to 14 after treatment at passage 0 with complex **16** (2 μM, 20 min). (b) The integrated intensity of the self-assembled complex in lysosomes of 1 to 15 cell generation. (c) LSCM images of HeLa cells at passage 4, 9 and 14 after the same treatment as in (a). Reproduced with permission from ref. 62.

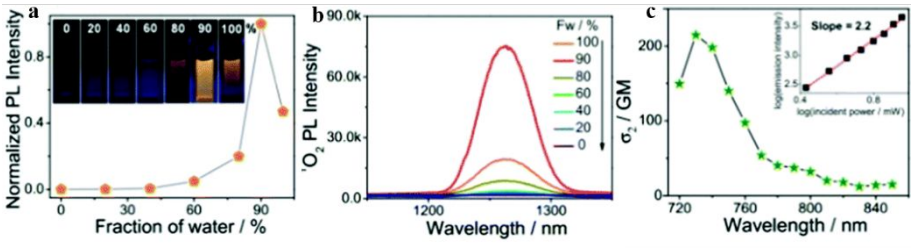

Fig. 6 (a) Normalised emission intensity of complex **30a** in solutions with different water fraction. (b) Emission spectra of $^1O_2$ in the presence of complex **30a** in varying fractions of water–DMSO mixture upon photoirradiation (λ_{ex} = 405 nm). (c) TPA cross-sections of complex **30a**. Inset: logarithmic dependence of emission intensity on incident power. Reproduced with permission from ref. 88.

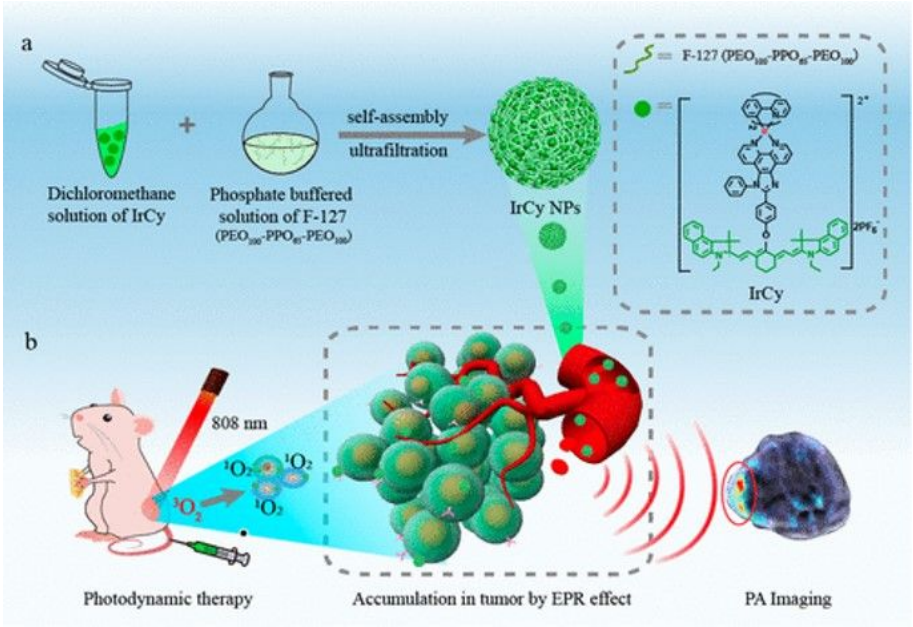

Fig. 7 Schematic illustration of (a) the fabrication of IrCy nanoparticles and (b) their application in photoacoustic guided PDT *in vivo*. Reproduced with permission from ref. 91.

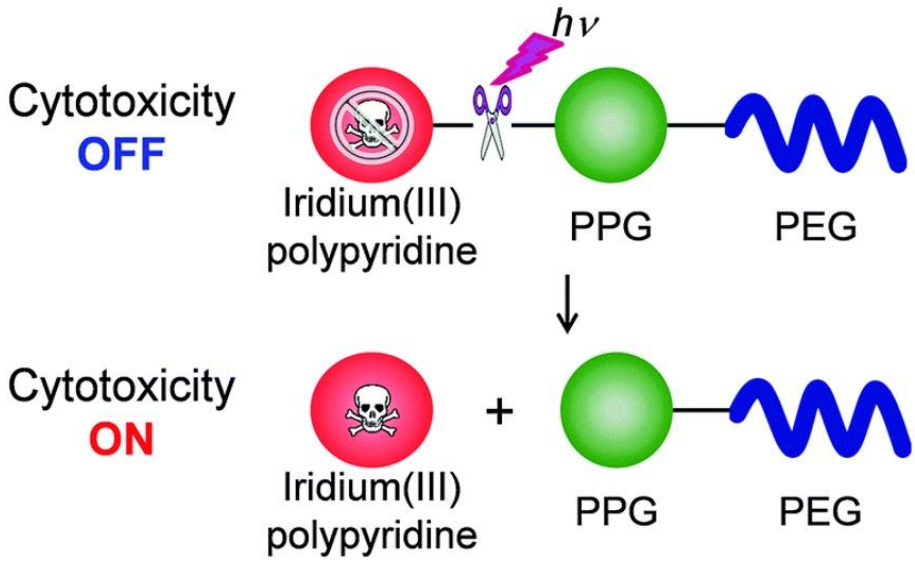

Fig. 8 Schematic illustration of the photorelease of complex **35a**. Reproduced with permission from ref. 111.

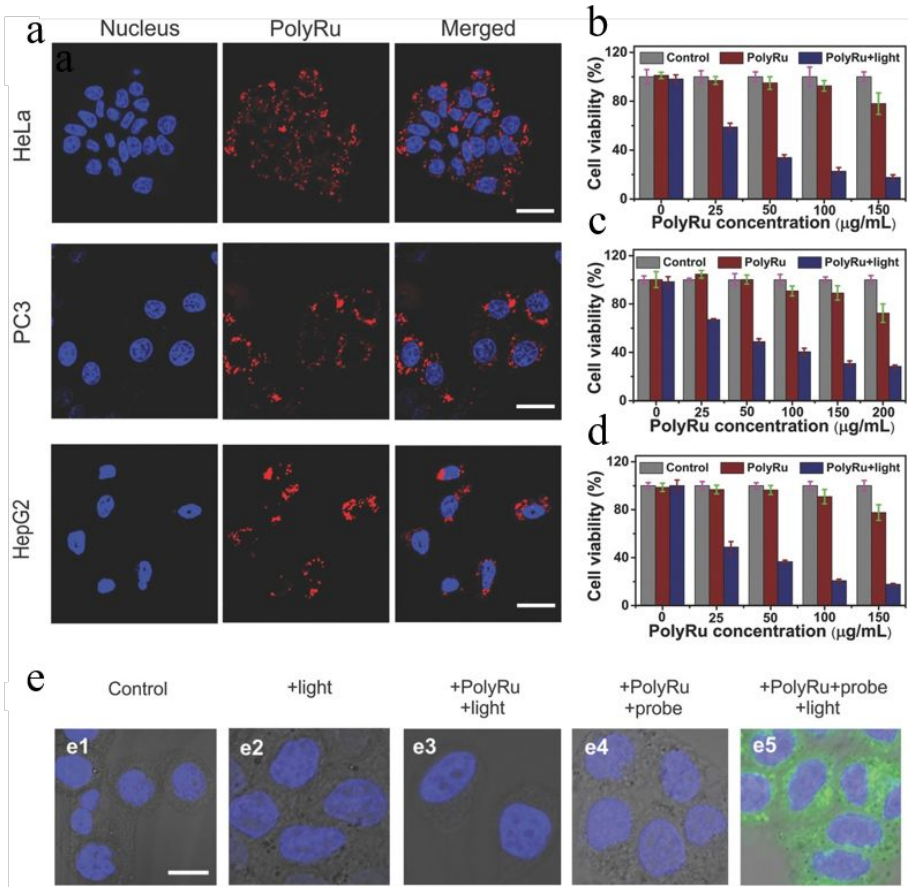

Fig. 9 (a) LSCM images of HeLa cells (first row), PC3 (second row), and HepG2 (third row) incubated with PolyRu nanoparticles (red) for 6 h or Hoechst 33342 (blue). Viability of (b) HeLa, (c) PC3 and (d) HepG2 cells incubated with PolyRu nanoparticles at various concentrations in the dark and after red light irradiation (656 nm, 50 mW cm^{-2}, 30 min). (e) LSCM images of HeLa cells (1) without and (2) with photoirradiation; (3) incubated with PolyRu nanoparticles followed by photoirradiation; incubated with PolyRu nanoparticles and $^1O_2$ probe (4) without and (5) with photoirradiation. Reproduced with permission from ref. 113.

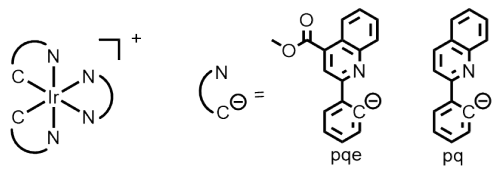

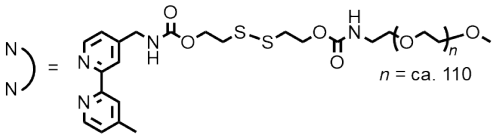

N^C = pqe **1a**
pq **2a**

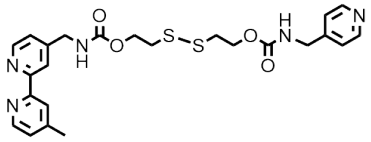

N^C = pqe **1b**
pq **2b**

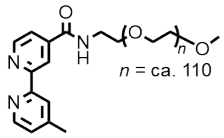

N^C = pqe **1c**
pq **2c**

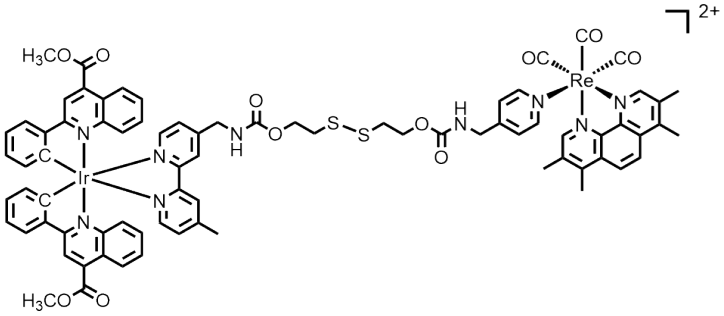

3

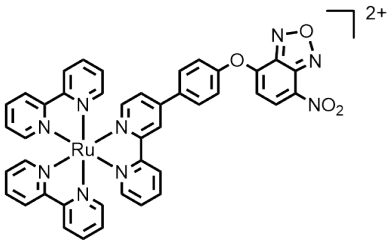

4

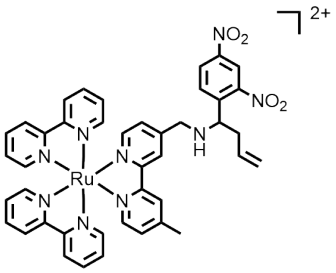

5

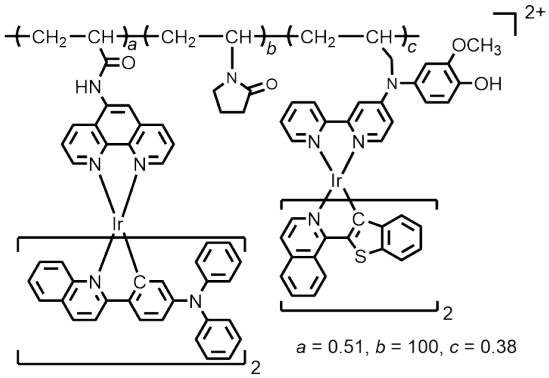

a = 0.51, *b* = 100, *c* = 0.38

6

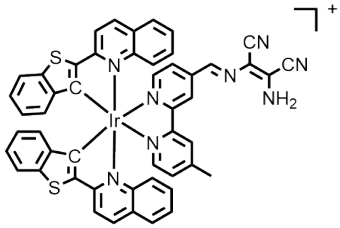

7

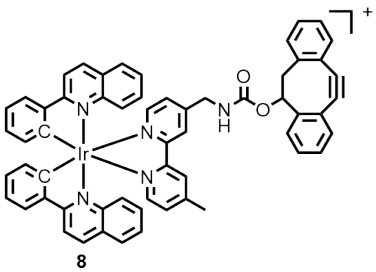

8

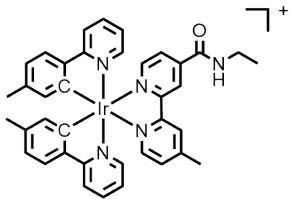

9a

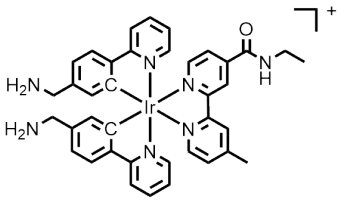

9b

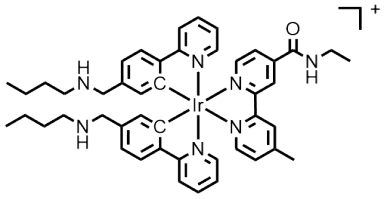

9c

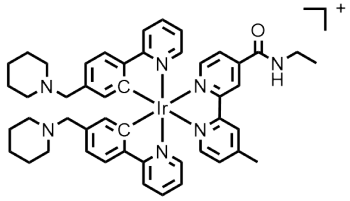

9d

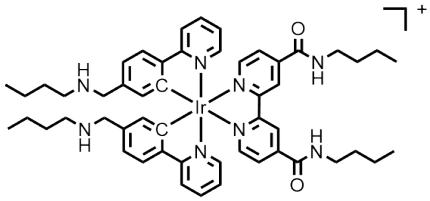

9e

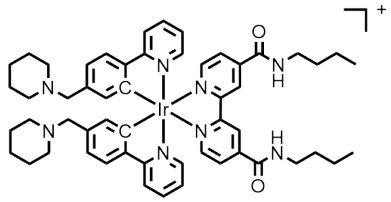

9f

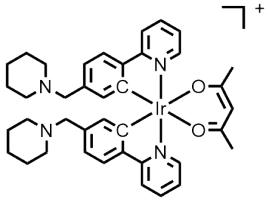

9g

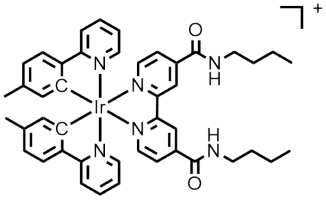

9h

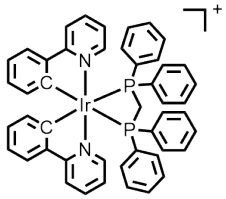

10a

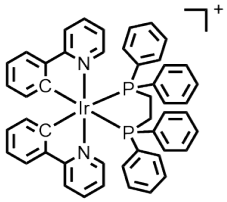

10b

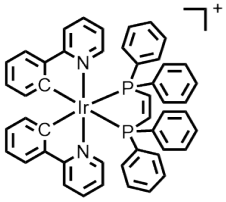

10c

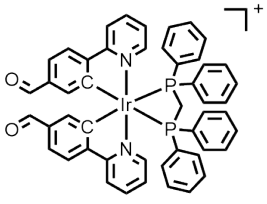

10d

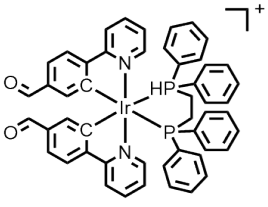

10e

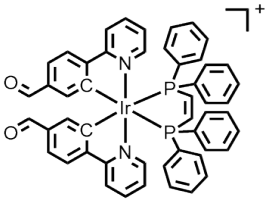

10f

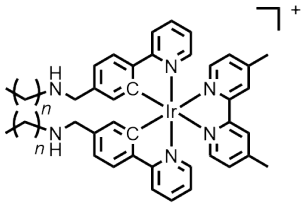

n = 3 (**11a**) 5 (**11b**) 7 (**11c**) 9 (**11d**)

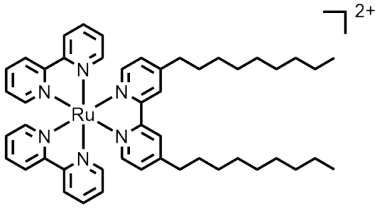

12

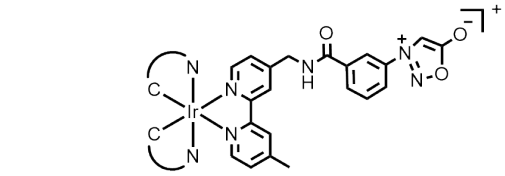

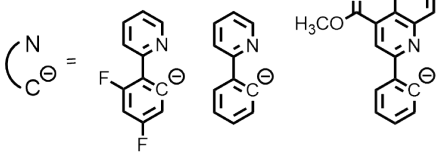

13a **13b** **13c**

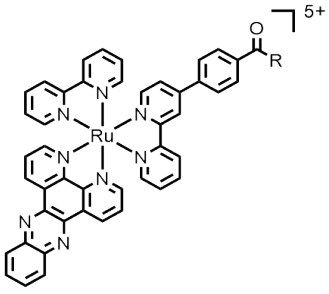

R = –NH-ahx-FrFKFrFK(Ac) (**14**)

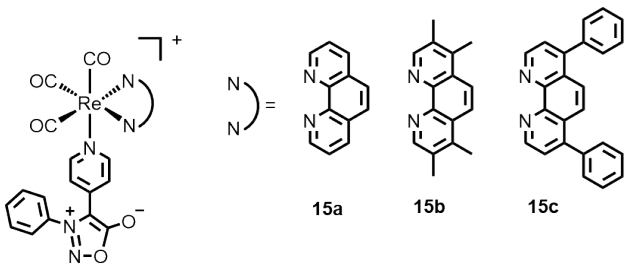

15a 15b 15c

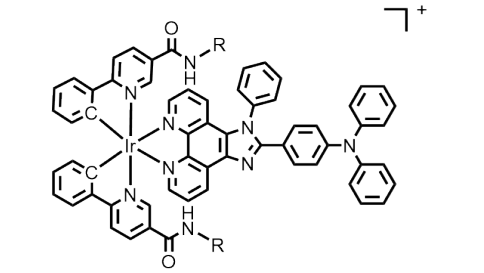

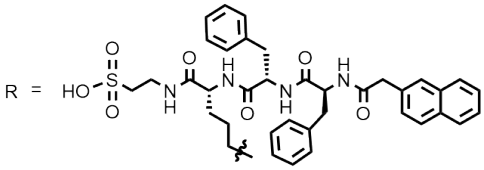

16

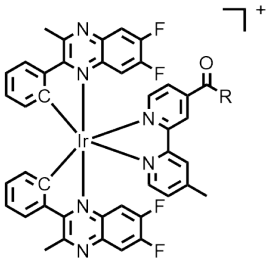

17a

17b

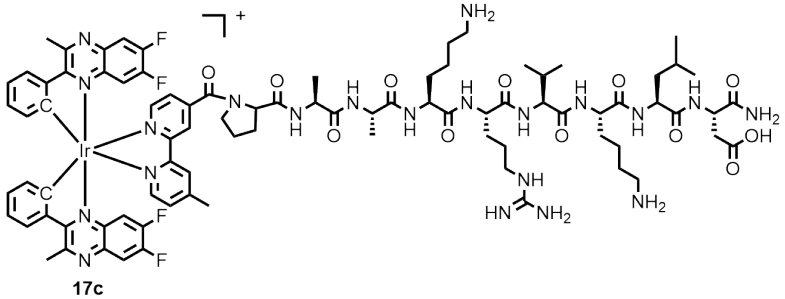

17c

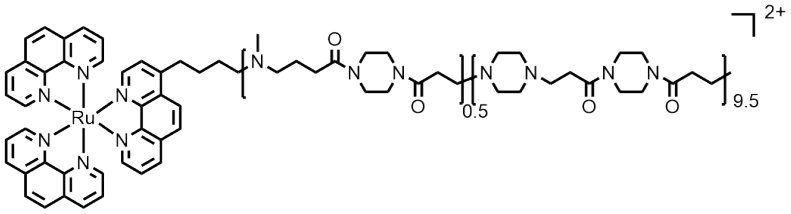

18

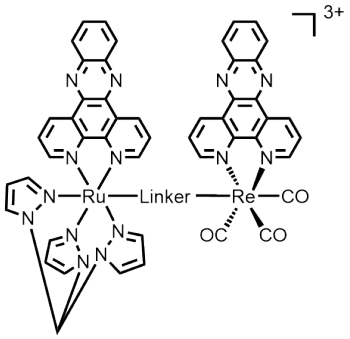

Linker =

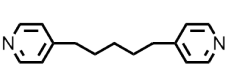

19a

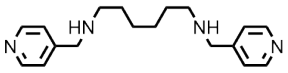

19b

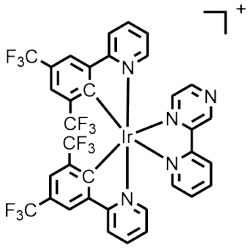

20a

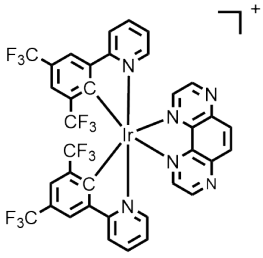

20b

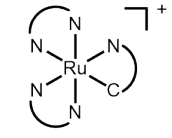

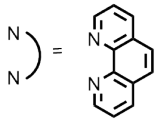

phen

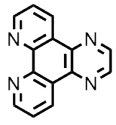

dpq

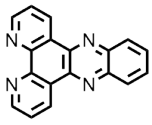

dppz

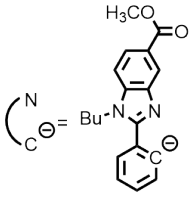

N^N = dpq (**21a**)

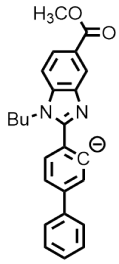

N^N = dpq (**21b**)
phen (**21d**)
dppz (**21e**)

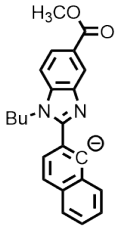

N^N = dpq (**21c**)

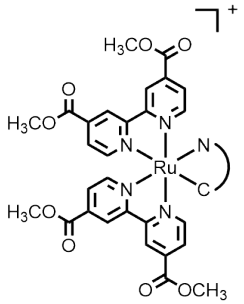

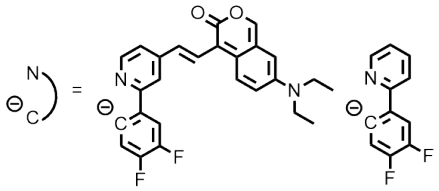

22a **22b**

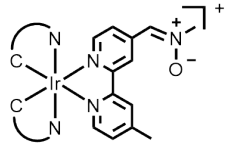

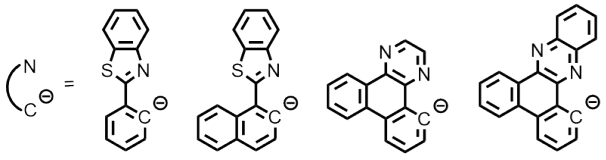

23a **23b** **23c** **23d**

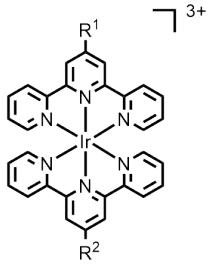

$R^1 = R^2 =$ Ph	**24a**
R^1 =4'-$N(CH_3)_2$Ph, R^2 = Ph	**24b**
$R^1 = R^2$ = 4'-$N(CH_3)_2$Ph	**24c**
R^1 = Pyren-1-yl, R^2 = Ph	**24d**
$R^1 = R^2$ = Pyren-1-yl	**24e**
R^1 = 4'-$CH_3(OCH_2CH_2)_3$OPh, R^2 = Ph	**24f**

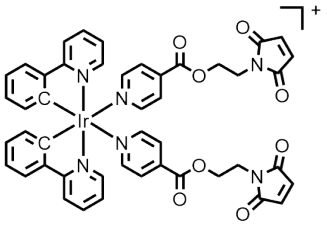

25

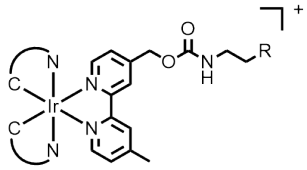

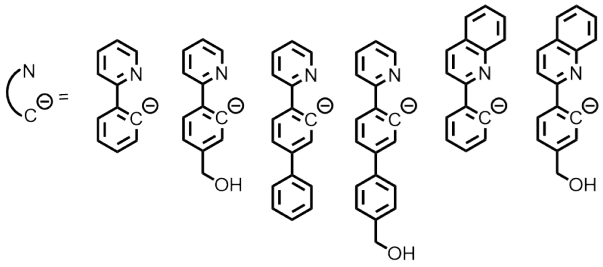

ppy ppy-CH_2-OH pppy pppy-CH_2-OH pq-CH_2-OH

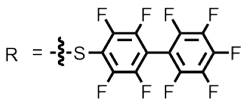

R = -§-CH_2CH_3

N^C =	ppy	**26a**
	ppy-CH_2OH	**26b**
	pppy	**26c**
	pppy-CH_2OH	**26d**
	pq	**26e**
	pq-CH_2OH	**26f**
N^C =	ppy	**27a**
	ppy-CH_2OH	**27b**
	pppy	**27c**
	pppy-CH_2OH	**27d**
	pq	**27e**
	pq-CH_2OH	**27f**

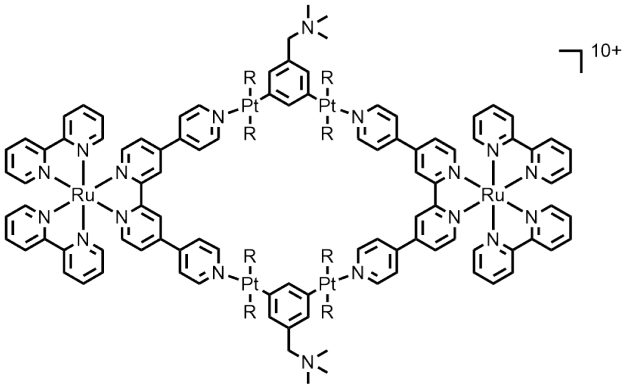

28

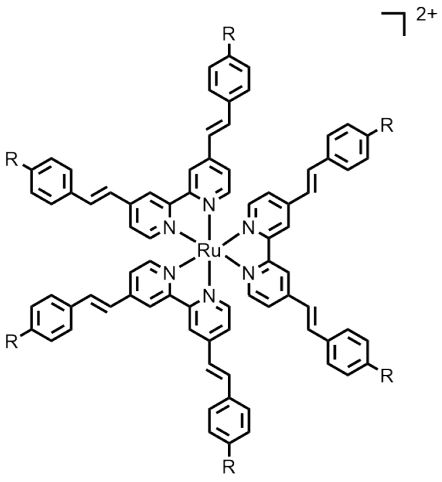

R = H **29a**

NMe_2 **29b**

OMe **29c**

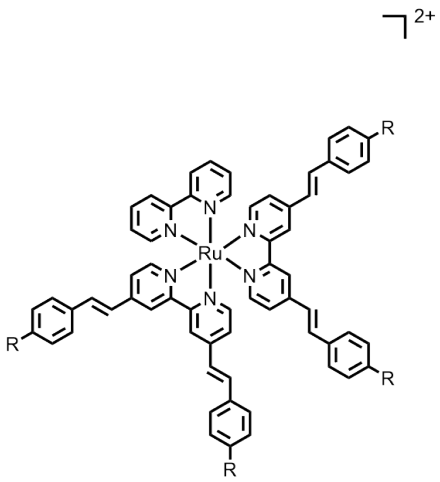

R = NMe_2 **29d**

OMe **29e**

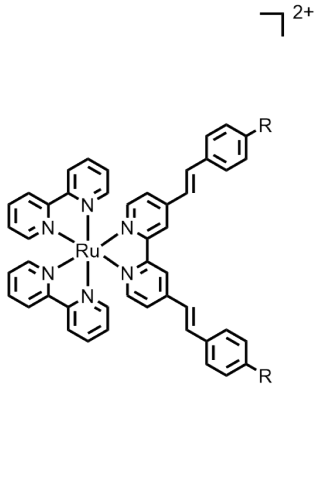

R = NMe_2 **29f**

OMe **29g**

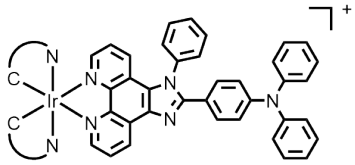

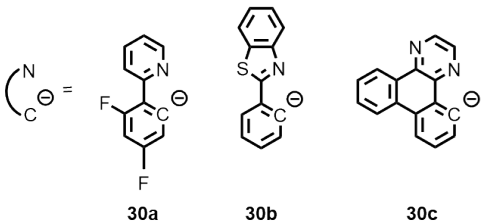

30a **30b** **30c**

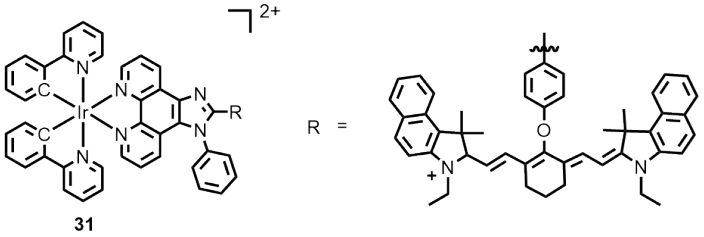

31

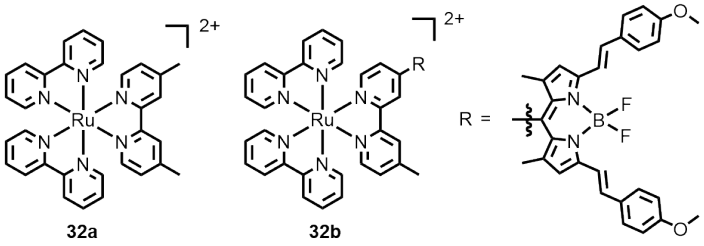

32a **32b**

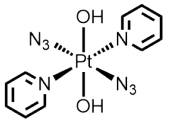

33

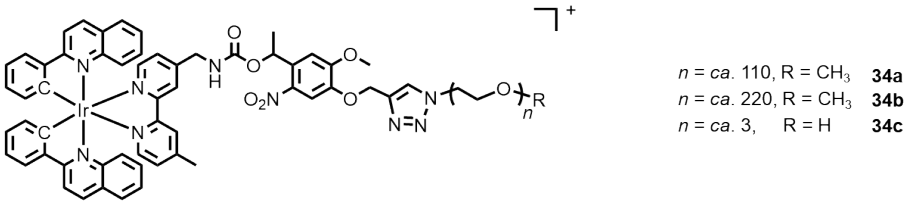

n = *ca.* 110, R = CH_3 **34a**
n = *ca.* 220, R = CH_3 **34b**
n = *ca.* 3, R = H **34c**

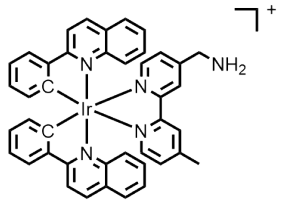

34d

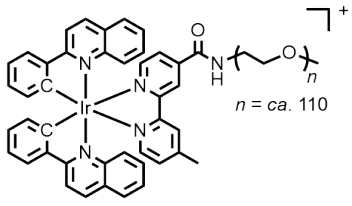

n = *ca.* 110

34e

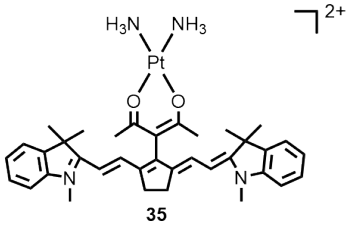

35

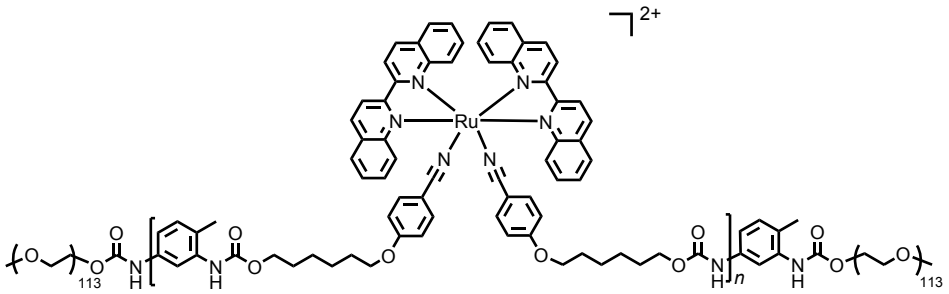

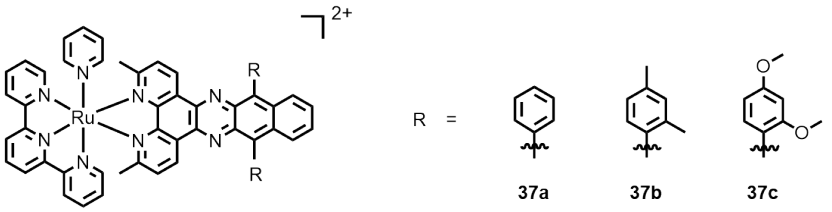

37a **37b** **37c**

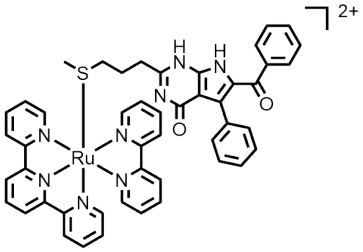

38

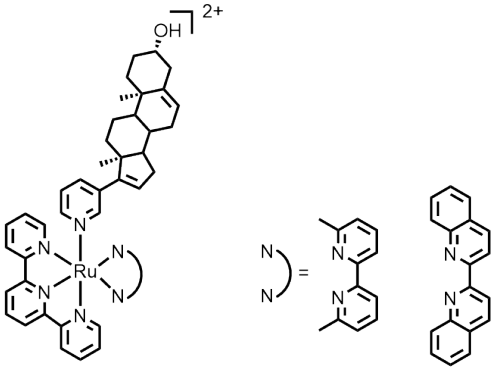

39a **39b**

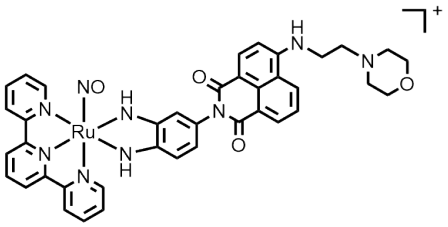

40

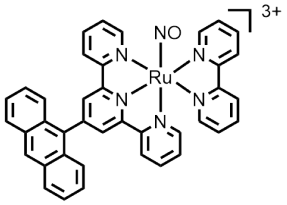

41

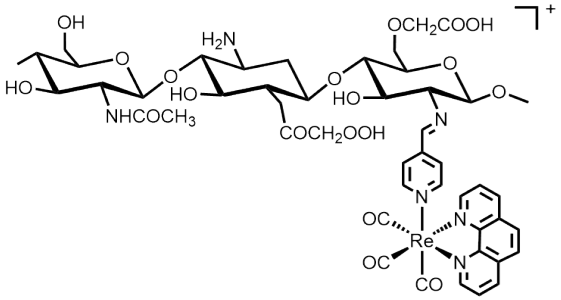

42

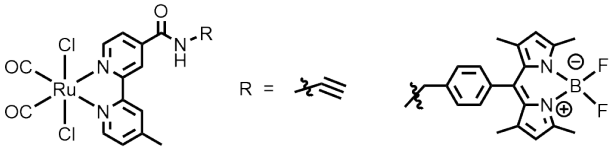

43a **43b**